

Modeling and Control of a Battery Connected Standalone Photovoltaic System

Thesis submitted in partial fulfillment of the requirements for the degree of

Master of Technology

in

Electrical Engineering

(Specialization: Control & Automation)

by

Priyabrata Shaw



Department of Electrical Engineering
National Institute of Technology Rourkela
Rourkela-769008, Odisha, India

May 2015

Modeling and Control of a Battery Connected Standalone Photovoltaic System

Dissertation submitted

in May 2015

to the department of

Electrical Engineering

of

National Institute of Technology Rourkela

in partial fulfillment of the requirements for the degree of

Master of Technology

by

Priyabrata Shaw

(Roll no-213EE3298)

under the supervision of

Prof. Somnath Maity



Department of Electrical Engineering
National Institute of Technology Rourkela
Rourkela-769008, Odisha, India

Dedicated
to
my loving parents and my elder brother Satya



Department of Electrical Engineering
National Institute of Technology Rourkela
Rourkela-769008, Odisha, India. www.nitrkl.ac.in

CERTIFICATE

This is to certify that the thesis entitled “*Modeling and Control of a Battery Connected Standalone Photovoltaic System*” by *Mr. Priyabrata Shaw* is a record of an original research work carried out by him under my supervision and guidance in partial fulfillment of the requirements for the award of the degree of Master of Technology with the specialization of “**Control & Automation**” in the department of **Electrical Engineering**, National Institute of Technology Rourkela. The research reports and the results embodied in this thesis have not been submitted in parts or full to any other University or Institute for the award of any other degree or diploma.

Place: NIT Rourkela
Date:

Prof. Somnath Maity
Dept. of Electrical Engineering
National Institute of Technology

Acknowledgment

First and Foremost, I would like to express my sincere gratitude towards my supervisor Prof. Somnath Maity for his advice during my project work. He has constantly encouraged me to remain focused on achieving my goal. His observations and comments helped me to establish the overall direction of the research and to move forward with investigation in depth. He has helped me greatly and been a source of knowledge.

I express my gratitude to Prof. Bidyadhar Subudhi, Prof. Sandip Ghosh, Prof. Susovan Samanta, and Prof. Susmita Das for their advice and care. I am also very much obliged to Prof. A. K. Panda Head of the Department of Electrical Engineering, NIT Rourkela for providing all the possible facilities towards this work.

I would also like to thanks Phd research scholars especially to Pradeep Kumar Sahu, Satyajit Das, and Sanjeet Kumar Subudhi for their help and moral support. I am really thankful to my batchmates especially Pawan and Abhilash who helped me during my course work. My sincere thanks to everyone who has provided me with kind words, new ideas, a welcome ear, useful criticism, or their invaluable time, I am truly indebted. I must acknowledge the academic resources that I have got from NIT Rourkela.

Last, but not the least, I would like to acknowledge the love, support and motivation I received from my family.

Priyabrata Shaw
213EE3298

Abstract

Nowadays, due to the decrease of conventional energy sources and growing problem of environmental pollution, renewable energy sources are playing a big role in producing electricity. Among them solar and wind are popular renewable energy sources, that have concerned with more and more attention. Solar energy has become a promising, popular and alternative source because of its advantages such as abundance, pollution free, renewability and maintenance free. This work is based on a standalone photovoltaic (PV) system in which a storage device is used as a backup source. The remote areas, which are isolated from utility grid, standalone operation of PV system is the best option. But due to diurnal cycle of the earth and weather condition, solar energy is not constant throughout the day and also sometimes the PV generation is not sufficient to fulfill the power demand of the varying local load. Hence PV system cannot give a steady power to the load connected in standalone PV system, which makes the system unstable. So the use of dedicated energy storage systems needs to be taken into account to make this intermittent PV power more dispatchable and stable. Here, the storage device is mainly taken as a lead-acid battery, as it is more convenient to use in high power applications such as solar and wind systems because of its low cost and availability in large size.

For controlling the standalone PV system, its mathematical modeling is very much necessary. So the modeling of PV system and lead-acid battery by using the corresponding equivalent circuits are discussed. As we know, to increase the efficiency of PV array maximum power should be extracted from it. Here an analog MPPT controller is used for extracting the optimal power available at PV module, by controlling the duty cycle of a boost converter. This analog MPPT control technique shows fast and robust behavior even in changing environmental and load condition compared to conventional MPPT control techniques. For charging and discharging of the lead-acid battery, a bidirectional buck-boost converter is

used, which is capable of transferring power in both the direction with appropriate voltage level. To provide electrical power to any load or appliances, the inverter converts the DC bus voltage to a single phase AC voltage with appropriate amplitude and frequency. In this work a current-controlled single phase VSI with bipolar pulse width modulation is used to maintain the stable voltage and current at local load. Thus here three independent control loops are used to control the whole standalone system. Those are MPPT control loop for extracting maximum power from PV module, battery control loop for bidirectional power flow between battery and DC-link through bidirectional buck-boost converter and inverter control loop for maintaining stable voltage and current at local load. The stability analysis is performed by using bode plots for both the inverter control loop and buck-boost converter control loop and these control loops are stable for our tuned controller parameters. The system is simulated in MATLAB/SIMULINK and simulation results shown to fulfill the objectives of the standalone PV system. The simulation results prove the effectiveness of the proposed controllers.

Contents

Certificate	iii
Acknowledgement	iv
Abstract	v
List of Figures	x
List of Tables	xii
Symbols and Abbreviations	xiii
1 Introduction	2
1.1 Overview	2
1.2 Background	2
1.3 Motivation	4
1.4 Objectives and Contribution of the Thesis	4
1.4.1 Objectives	4
1.4.2 Contribution of the Thesis	5
1.5 Literature Review	5
1.6 Organization of the Thesis	6
1.7 Summary	7
2 System Description and its Modeling	9
2.1 Overview	9
2.2 Photovoltaic System	9
2.2.1 Standalone PV System	10
2.2.2 Grid-Connected PV System	11
2.2.3 Hybrid System	11

2.3	PV Array	12
2.3.1	PV Modeling	13
2.3.2	Single module ratings use for simulation	14
2.3.3	Simulation results of one module	15
2.4	Battery	16
2.4.1	Battery Modeling	16
2.5	Boost Converter	18
2.6	Bidirectional DC DC converters	18
2.7	Single Phase Inverter	20
2.7.1	Half bridge inverter	20
2.7.2	Full bridge inverter	21
2.8	Filter	22
2.9	Sinusoidal Pulse Width Modulation (SPWM)	23
2.10	Load	24
2.11	Summary	24
3	Control Strategies and Analysis	26
3.1	Overview	26
3.2	Analog MPPT Control	26
3.2.1	Control Logic	28
3.3	Battery Control	30
3.3.1	State-Space Averaging of Bidirectional Buck-Boost Converter	31
3.4	Inverter Control	35
3.4.1	State-Space Averaging of Inverter	36
3.5	Summary	38
4	Results and Discussion	40
4.1	Overview	40
4.2	Simulation	40
4.3	Results and Discussion	41
4.3.1	At nominal condition	41
4.3.2	With load variation	43

4.3.3	With solar irradiance variation	45
4.4	Summary	48
5	Conclusion and Future Scope	50
5.1	Overview	50
5.2	Conclusion	50
5.3	Future Scope	51
5.4	Summary	51
	Bibliography	52

List of Figures

2.1	Battery connected standalone PV system	10
2.2	Standalone PV system with battery	10
2.3	Grid-connected PV system with battery	11
2.4	Battery connected hybrid PV system	12
2.5	PV cell, module and array	12
2.6	Equivalent circuit of solar cell	14
2.7	(a) $i - v$ curve (b) $p - v$ curve at different irradiation level	15
2.8	(a) $i - v$ curve (b) $p - v$ curve at different temperature level	15
2.9	Battery equivalent circuit	16
2.10	Simulation result of discharge characteristics	17
2.11	Data-sheet result of discharge characteristics	17
2.12	Boost or Step-up Converter	18
2.13	Non-isolated bidirectional buck-boost converter	19
2.14	Single phase half bridge inverter	21
2.15	Single phase full bridge VSI	21
2.16	Single phase full bridge CSI	22
2.17	LC filter with damping resistance	22
2.18	Bipolar sinusoidal pulse width modulation	23
3.1	P-V curve.	27
3.2	Analog MPPT controller with boost converter	27
3.3	Control strategy for buck-boost DC-DC converter	30
3.4	Equivalent circuit of PV module	31
3.5	Equivalent circuit with Q1-off, Q2-on	32
3.6	Equivalent circuit with Q1-on, Q2-off	32
3.7	Control block diagram for battery	34
3.8	Bode diagram for current loop ($Li1$) of buck-boost converter	34
3.9	Bode diagram for voltage loop ($Lv1$) of buck-boost converter	35
3.10	Control strategy for single phase VSI	35
3.11	Control block diagram for inverter	37
3.12	Bode diagram for current loop ($Li2$) of inverter	38
3.13	Bode diagram for voltage loop ($Lv2$) of inverter	38
4.1	Steady state output voltage (V_0)	41
4.2	Steady state load current (i_0)	41
4.3	Steady state DC-link voltage (V_{dc})	42
4.4	Steady state SOC of battery system	42
4.5	Steady state PV voltage at MPP (V_{mpp})	42
4.6	Steady state PV current at MPP (I_{mpp})	43

4.7	Output voltage (V_0) under load variation	43
4.8	Load current (i_0) under load variation	44
4.9	PV, output load and battery power under load variation	44
4.10	SOC of battery system under load variation	44
4.11	Power management protocol under solar irradiance variation	45
4.12	Output voltage (V_0) under solar irradiance variation	46
4.13	Load current (i_0) under solar irradiance variation	46
4.14	PV, output load and battery power under solar irradiance variation	46
4.15	SOC of battery system under solar irradiance variation	46
4.16	V_{mpp} under solar irradiance variation	47
4.17	I_{mpp} under solar irradiance variation	47

List of Tables

2.1	Single Module Ratings	14
3.1	Principle of operation of MPPT controller	29

List of Abbreviations

PV	: Photovoltaic
DPGS	: Distributed power generation systems
RAPS	: Remote area power supply
D	: Duty ratio
MPPT	: Maximum power point tracking
DC	: Direct current
AC	: Alternating current
SOC	: State of charge
EMI	: Electromagnetic interference
MPP	: Maximum power point
PWM	: Pulse width modulation
SPWM	: Sinusoidal pulse width modulation
VSI	: Voltage source inverter
CSI	: Current source inverter
Hz	: Hertz
BJT	: Bipolar junction transistor
MOSFET	: Metal oxide semiconductor field effect transistor
IGBT	: Insulated gate bipolar transistor
kW	: Kilowatt
GW	: Gigawatt
RHS	: Right hand side
BSS	: Battery storage system

Chapter 1

Introduction

Chapter 1

Introduction

1.1 Overview

The chapter 1 gives an overall background and the purpose of this research work. Section 1.2 gives brief idea about the purpose of this work. Section 1.3 describes the motivation of this work. The objectives and the contribution to the research work is described in Section 1.4. The literatures are based on the standalone PV system, grid-connected PV system, PV modeling and battery modeling are discussed in Section 1.5. Finally, the chapter concludes with the organization of this thesis in Section 1.6.

1.2 Background

A developing country like India has more energy demand compared to other countries. Nowadays, most of the energy comes from fossil fuels such as coal, diesel, petrol and gas, which is 80% of our current energy production. This energy demand is expected to rise by almost half over the next two decades. Possibly this is causing some fear that our energy resources are starting to run down, which has very serious disturbing consequences on the global quality of life and global economy. This increasing demand of energy has two major impacts like energy crisis and climate change. Also the greenhouse gas production related to energy increases due to rise in energy demand. Globally it is a challenge to reduce the CO_2 emission and offer sustainable, clean and affordable energy. Energy saving is one of the best cost effective solution for the worldwide increasing energy demand but does not tackle perfectly till now. For that issue, renewable energy is a good option because it gives a green and clean energy free of CO_2 emission. Renewable energy is defined as the energy that comes from resources which are naturally generated like sunlight, wind, rain, tides, waves and geothermal heat. In recent years, the development on alternative energy sources has become a global priority which giving rise to intensive research about these available renewable energy technologies such as PV, hydroelectric, wind, geothermal, and tidal systems. So due to the growing problem of environmental pollution and decrease of conventional energy sources, the utilization and research of the renewable energy sources, such as solar energy, wind energy has concerned with more and more

attention. And among all renewable energy sources solar power is very much popular for its environmental-friendly features and plug-N-play operation.

Solar energy has become a promising, popular and alternative source because of its advantages such as abundance, pollution free, renewability and maintenance free. PV system requires less maintenance as compared to wind, hydroelectric and tidal systems because all these systems require rotating instrument for energy conversion which is not required for conversion of solar energy to electrical energy. In late 1950s the first conventional PV cells were produced and throughout the next ten years PV cells were mainly used for providing electrical power for earth-orbiting satellites. In the 1970s the cost of PV modules reduced due to the improvements in its manufacturing, quality and performance. The reduction in cost opened up various opportunities for powering remote terrestrial applications which includes battery charging for navigational systems and other critical low-power requirements. In the 1980s, PV became a very popular source of power for consumer electronic devices like calculators, radios, watches, lanterns and for other small battery-charging applications. After the energy crises of the 1970s, a significant development started in PV power systems for commercial and residential uses, for both standalone as well as grid-connected applications. During this period, due to the dramatic increase of international applications for PV systems to power the rural health clinics, refrigeration, water pumping, telecommunications, and other off-grid households, it remains a major portion of present world market for the photovoltaic products.

Nowadays, production of PV modules is growing at approximately 25% per year, and the implementation of PV systems on buildings and interconnection to utility networks are rapidly increasing and become major programs of developed countries like Japan, U.S. and Europe. This PV system has been used for over 50 years in various specialized applications and grid-connected PV systems have been in use for over 20 years. PV installed capacity had increased approximately to 177 GW worldwide in 2014. That is sufficient for supplying 1% of electricity demand globally. So the approximately 200 GW capacity of PV power is installed till date which is 40 times the installed capacity of 2006. Worldwide, maximum PV systems are utility connected where large amount of PV capacity is involved. But for remote areas, which are isolated from utility grid, standalone operation is the best option. Due to diurnal cycle of the earth and weather condition solar energy is not continuous and constant throughout the day. And also sometimes the PV generation is not sufficient to fulfill the power demand of the varying local load. Hence PV system cannot give a steady power to the load connected, which makes the system unstable as in standalone system solar is the only source of energy. However, the use of energy storage systems needs to be taken care of because of the discontinuous or intermittent nature of the PV generation as they are highly influenced by natural and meteorological conditions. So we can make this intermittent PV power more dispatchable and stable by using storage devices. Among all available storage devices like batteries, ultra-capacitors, compressed air systems, etc., batteries have the highest importance in PV system as they store energy through the electrochemical process and thus have quick response in

both charging and discharging processes. Also battery has high power and energy density which makes it one of the most suitable technology, used to bridge the power fluctuations generated from PV systems.

1.3 Motivation

Due to the rapidly increasing energy demand from the commercial and industrial sectors, especially in the current scenario of high oil prices, steadily reducing energy sources and increased concerns about environmental pollution, renewable energy based distributed power generation systems (DPGS) are gaining more importance. Especially solar energy is noise free, pollution free and readily available source of energy than other available renewable energy sources.

The major problem with solar energy is poor conversion efficiency and high installation cost. So research going into this area to develop the efficient control mechanism to provide better operation and control. Worldwide, maximum PV systems are utility connected where large amount of solar power is involved. But due to difficulties in maintaining transmission lines and equipment on isolated islands or remote coastal regions, it is also often difficult to maintain long distance transmission of electrical supplies for utility and domestic purposes. Hence, the use of local generation is often considered as the most convenient and cost effective solution. But due to intermittency nature of solar energy, PV power cannot meet the load demand and that requires a storage device which can solve this problem by its charging and discharging process if it is properly controlled. So the control and operation of a standalone PV system is very important and challenging for the electrical researchers. This challenging problem is the primary motivation of the following research work.

1.4 Objectives and Contribution of the Thesis

1.4.1 Objectives

In standalone PV system as solar is the only source of energy, battery is used to achieve the following objectives.

- To maintain the power balance between generation and demand.
- To supply power to local load at a regulated voltage by suppressing the transient that may occur in PV system due to source or load variation.
- To achieve fast dynamic performance under wide source and load fluctuation.
- To store electrical energy when there is an excess is available and to provide it when required.
- To supply power to the local load for a short time during peak hours.

1.4.2 Contribution of the Thesis

The primary objective of this work is to model, control and analyze a standalone PV system. Some of the salient points of this thesis are:

1. Description of the components of standalone PV system.
2. Modeling of PV module and lead-acid battery.
3. Design of a analog MPPT controller for boost DC-DC converter.
4. Control of a bidirectional buck-boost DC-DC converter for maintaining continuous power flow between the DC bus and battery storage with a constant DC-link voltage.
5. Implementation of current control strategy for single phase voltage source inverter.
6. Stability analysis of the system by using Bode diagram.

1.5 Literature Review

A PV system uses solar cells to directly convert the solar energy into electrical energy. Simply we can say PV systems are like any other electrical power generating systems, but the equipment used for PV system is different than that used for conventional electro-mechanical generating systems. However the principles of operation and method of interfacing with other electrical systems remain the same. Mainly PV systems are operated in three modes called standalone mode, grid-connected mode, and hybrid mode [1]. We know nowadays maximum PV systems are utility connected but in remote areas where utility supplies are not available, standalone PV systems are very popular. In standalone PV system solar power is only the source of power and the intermittency issue of solar power can be addressed by introducing storage element to the system [2]. This storage device or battery is very crucial in standalone PV system for maintaining power balance between PV generation and load demand [1, 2]. This type of system creates a hybrid PV/battery system which is capable of providing steady power to the load. In other hand, storage device like battery is not a critical element of grid-connected PV systems, though sometimes it can be used to reduce PV power fluctuations, perform peak shaving and supply emergency power [3, 4]. In A grid-connected PV system, li-ion batteries as backup power supply is used to support the voltage and frequency support through active and reactive power compensation. And the system will able to maintain balance between demand and supply of active and reactive power at any given point of time [5]. Various control strategies of a grid-connected and islanded PV microgrid are studied. These control technique are the MPPT control, and voltage-frequency control to provide voltage and frequency support to an islanded microgrid [6]. These control strategies are also useful for control of standalone PV system. The main components of standalone PV systems are PV module, battery and local loads [7], which need to be well understood for its modeling and control. Among all

available storage devices, battery is most suitable for renewable energy application as they have high power and energy density compared to other. And Lead-acid battery is more appropriate for renewable energy application like solar and wind because of its low cost, availability in large size and more mature with recycling at end-of-life. For controlling the PV system its modeling is very much necessary for the researchers and it has to give highest importance. So modeling of PV system is a vital part of this work. Here for system simulation the PV system is modeled using its equivalent circuit and equations [8]. In 1994, J. B. Copetti presents a new normalized model with a battery capacity that shows reasonable agreement with actual data [9]. The study focuses on the lead-acid batteries, because at present these are the most commonly used batteries in PV application owing to their relatively low cost and wide availability. In 2009 Olivier Tremblay has validated the dynamic model of batteries by simulating the discharge curve of battery at constant current [10]. He also presented the charging and discharging models of various batteries like lead-acid, li-ion, nickel-cadmium etc. Simultaneously in another paper he validated the dynamic model of batteries by simulating the discharge curve of battery at constant current [11]. Qiu Bin [12] presented control methods of the converters in the system and power management strategies of a standalone PV system and he discussed it with appropriate experimental results. The analysis, design and simulation methods of a photovoltaic energy management system with battery backup is reviewed [13] that gives the idea about system and its control methodology. This proposed system is capable of both grid-connected and islanded operation. For this work modeling, control and simulation of islanded PV system is very much useful. As battery is a cost effective source compared to other, we should not use battery where we will get less power but it will cost more compared to utility power. So it is required to find the size of the battery storage for the system in which it is being used [14]. The method of determining the size of battery storage used in grid connected PV system is studied.

1.6 Organization of the Thesis

The thesis work has been organized as follows:

- **Chapter 2:** provides a brief description about the standalone PV system, its components and the modeling of PV system and lead-acid battery.
- **Chapter 3:** deals with the description and implementation of all the control strategies and their stability analysis.
- **Chapter 4:** contains all the simulation results and its discussion under load and solar power variation.
- **Chapter 5:** presents the conclusion about the standalone PV system along with the future research scope.

1.7 Summary

This chapter has introduced solar energy and discussed about PV system and its importance in modern society. It has also discussed about the problems regarding the PV system and especially about the problems which needs to be taken care of in a standalone PV system. It has briefly highlighted the motivations, discussed about the objectives of this work and our contribution to fulfill that objective. The literature about the PV system, battery, their modeling and control are studied and discussed. Finally, the thesis structure and its organization are briefly outlined towards the end.

Chapter 2

System Description and its Modeling

Chapter 2

System Description and its Modeling

2.1 Overview

The chapter 2 gives an overall idea about the PV system and its modeling. The description about all the components of the standalone PV system is given in this chapter. Section 2-2 gives brief idea about the photovoltaic system and its types. Section 2-3 describes the fundamental concepts about PV array and in this section also modeling of PV array is described. The conceptual overview about battery and its modeling is described in Section 2-4. Section 2-5 gives a fundamental idea about boost DC-DC converter. For battery charging and discharging, bidirectional buck-boost converter is essential. So in Section 2-6, details about bidirectional buck-boost converter and its working is described. Section 2-7 gives a fundamental description about the single phase inverter. Section 2-8 and Section 2-9 give brief description about filter and sinusoidal pulse width modulation technique respectively. And the chapter concludes with the Section 2-10, that gives some fundamental idea about load.

2.2 Photovoltaic System

The word photovoltaic is composed of two terms, "photo" means light and "voltaic" means voltage. Solar energy is directly converted into electrical energy by using solar cells. Simply we can say PV systems are just like any other electrical power generating systems, but the equipment used for PV system are different than that used for conventional generating systems. But the principles of operation and method of interfacing with other surrounding electrical systems remain the same. PV array produces electric power when exposed to sunlight but still a number of interfacing components are required to properly convert, conduct, control, distribute, and store the electric energy produced by the PV array. Depending on the operational and functional requirements of the system, the specific components required such as a DC-DC power converter, a DC-AC power inverter, battery bank along with its controller, supplementary energy sources and the specified electrical load or appliances. A standalone PV system is shown in Figure 2.1, along with

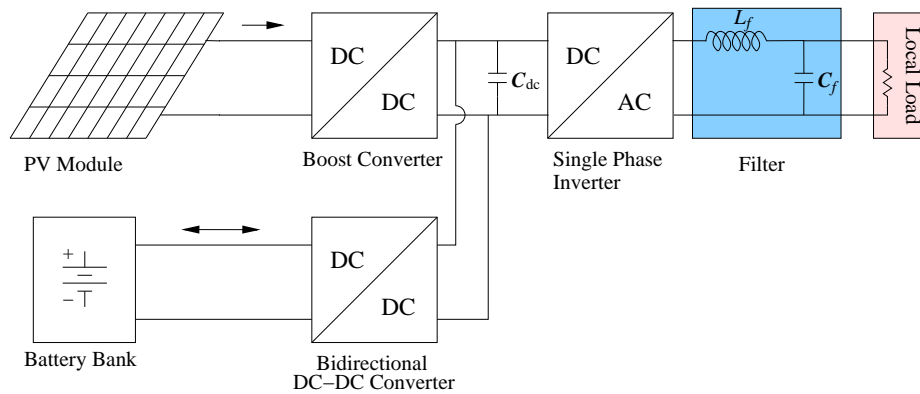


Figure 2.1: Battery connected standalone PV system

battery backup, all the interfacing components like DC-DC converter and DC-AC inverter, and local load. PV systems are mainly design to give the electric supply to load and load can be AC type or DC type. Supply for load or appliances can be needed in day time or evening time or both time. PV system can supply only in day time and for supply required during night hours, we require batteries, where power can be stored and utilized [15].

Types of PV System

Mainly PV systems are operated in three modes called standalone mode, grid-connected mode, and hybrid mode which are described below.

2.2.1 Standalone PV System

Where a utility power grid is not available or cannot be afford at reasonable costs, a standalone PV system can be used to generate the needed electric energy. Best examples for such cases are solar-powered water pumps, cabins in remote areas, emergency telephones, and also for boats or recreational vehicles. It is an off-grid electricity system and also known as remote area power supply (RAPS). As the solar modules produce electric power only during daytime, it is very much necessary to store the energy for night or for cloudy days. In renewable

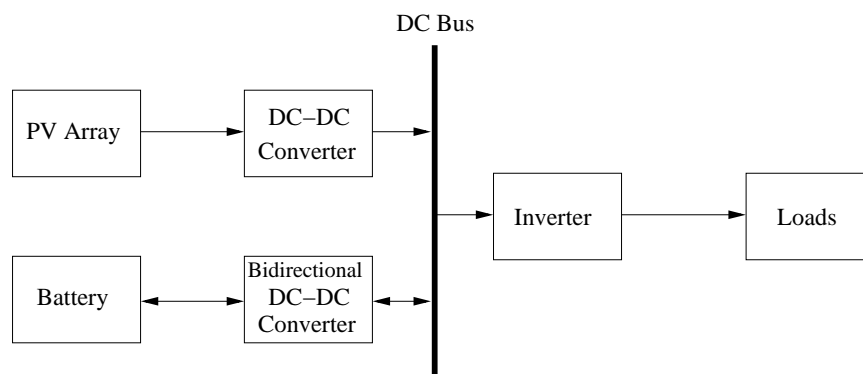


Figure 2.2: Standalone PV system with battery

applications like solar and wind, such storage system mostly uses rechargeable lead-acid batteries, due to their low cost, availability in large size and ability to accept with high efficiency for any input voltages. Mainly a battery regulator is used to prevent overcharging and a load shedding circuit is used to prevent deep discharges. Sometimes also fuel cells are used as the storage element in PV systems. In this type of system an inverter is used to generate AC voltage, in which more typical appliances can be used. In Figure 2.2 a basic block diagram of standalone PV system with battery as storage element is shown.

2.2.2 Grid-Connected PV System

Mainly grid-connected PV system is a special type of electricity generating PV system that is connected to the utility power supply. A grid-connected PV system consists of solar panels, one or more inverters, a power conditioning unit and grid connection equipment. These systems range from small residential and commercial systems to large utility scale solar power stations. Unlike standalone power systems, a grid-connected system rarely includes battery storage, as they are still very expensive. The grid-connected PV system supplies the excess power to the utility grid, beyond the consumption by the load, when conditions are all right. Figure 2.3 shows the block diagram of a grid-connected PV system. Grid connected system deals with very high power applications, so it is tough to store this much of power in battery. [16]

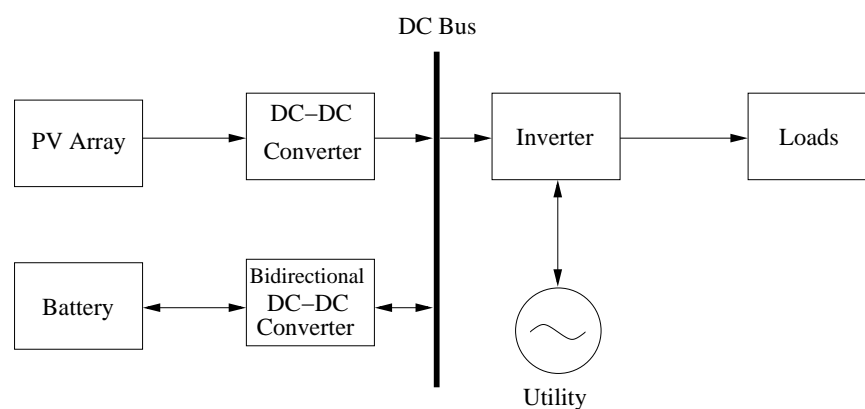


Figure 2.3: Grid-connected PV system with battery

2.2.3 Hybrid System

A "hybrid" is something that can be formed by combining two kinds of different components that produce the similar results. When PV system is use in conjunction with diesel generator, wind generator, micro turbines, fuel cells etc., system is called hybrid system. Figure 2.4 shows the block diagram of a Hybrid system. Hybrid PV systems most commonly formed by combining photovoltaic systems with wind turbines or diesel generators. These Hybrid systems are most likely be found on islands, nowadays they could also be built in other areas. A PV-diesel hybrid system ordinarily consists of a PV system, diesel generator sets

and intelligent management for ensuring the amount of solar energy fed into the system exactly matches the load demand at that time.

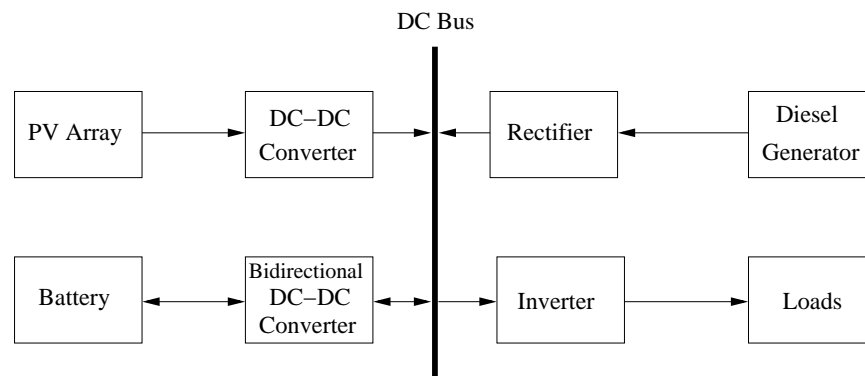


Figure 2.4: Battery connected hybrid PV system

2.3 PV Array

PV array consist of several modules, modules made of cells and each PV cell generates approximately 2 W of electric power. Generally, PV cells are connected electrically in series and/or parallel to produce higher voltages and currents respectively that ultimately results higher power levels. Sometimes PV panels may include one or more PV modules assembled as a pre-wired field-installable unit. A PV array is the complete power-generating unit, consisting of any number of PV modules and panels. Figure 2.5 shows the structure of PV cell, module and array.

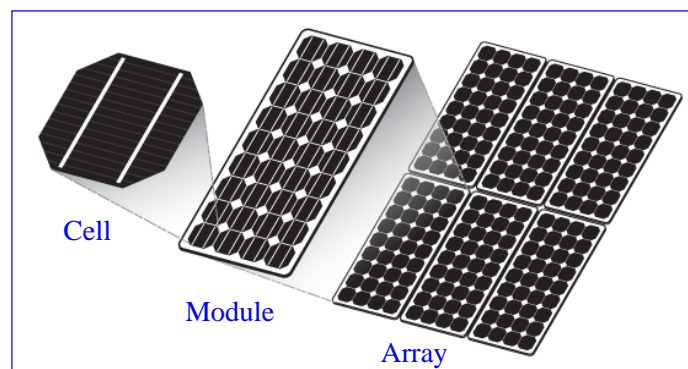


Figure 2.5: PV cell, module and array

Photovoltaic cell

PV cells (also called a solar cell) are sealed in an environmentally protective laminate to form a PV module, and are the fundamental building blocks of PV systems. The most common type of solar cell is made from silicon doped with

minute quantities of boron, gallium, phosphorous, arsenic, or other important materials. As it is made up of semiconductor, when light strikes to its surface electrons get knocked off and they collected from the metal connected to this cell. Generally each cell develops about half a volt of DC electrical potential when it is exposed to light. The maximum amperage of the cell depends on the intensity of the light and is proportional to its surface area exposed to light.

Photovoltaic module

PV module is also sometimes called as a panel and is nothing but a group of cells. Generally cells are more connected in series to increase the voltage rating of the PV module. Historically, modules with 36 cells have been most common and well known, producing 18 to 22 volts for a 12 volt nominal output. Power generated by a cell is very less so more number of cells connected in series to increase the power rating by increasing the voltage rating. A diode can be connected in antiparallel way to avoid the damage caused by partial shading.

Photovoltaic array

The term array describes as a group of modules in a single system. When power generated by a module is not sufficient for some applications, module can be connected in series or parallel, to meet desire ratings. Sometimes solar string is also commonly known as sub-array. But at some times, sub-array mainly used to mean that one rack of modules are in a multiple-rack array.

2.3.1 PV Modeling

For modeling of PV array, the mathematical equations are utilized [8, 17]. The characteristic equations of voltage and current are modeled using Matlab Simulink, given as follows. The electrical equivalent circuit of a PV cell is shown in Figure 2.6 that is very much required for its modeling. It includes a current source (I_{ph}) in parallel with a diode (D), a shunt resistance (R_{sh}) and a resistance (R_s) in series. The current output of PV module is

$$I_{pv} = N_p * I_{ph} - N_p * I_s \left[\exp \left(\frac{V_{pv}/N_s + I_{pv}R_s/N_p}{V_t a} \right) - 1 \right] \quad (2.1)$$

Where I_{pv} and V_{pv} are the current and voltage generated by the solar cell, I_{ph} is the current generated due to light or photocurrent, I_s is the saturation current, R_{sh} is the shunt equivalent resistance, R_s is the series equivalent resistance, $a (= 1.0)$ is an ideality factor and $V_t = n_s k T / q$ is the thermal voltage of PV array. Then $q (= 1.6 \times 10^{-19} C)$ is the charge of electron and $k (= 1.3806 \times 10^{-23} J/K)$ is the Boltzmann's constant. N_s and N_p are the series and parallel number of cells for a PV array respectively. For single module simulation $n_s = 36$, $N_s = 1$ and $N_p = 1$ are taken. The photo current mainly depends on the solar irradiance and cell temperature. That means when intensity of light and/or the corresponding temperature of the module changes, the current generated by the module also

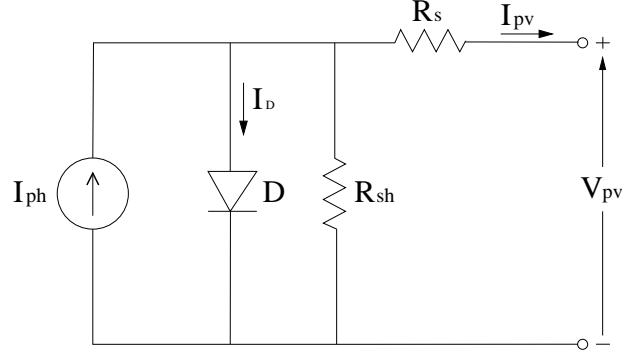


Figure 2.6: Equivalent circuit of solar cell

changes according to the following equation.

$$I_{ph} = [I_{pvn} + K_I(T - T_n)] \frac{G}{G_n} \quad (2.2)$$

Where I_{pvn} is the nominal light generated current, K_I is the short circuit current or temperature coefficient, T and T_n ($= 25^\circ C$ or $298K$) are actual and nominal temperature respectively, G is the irradiation level on module surface and G_n ($= 1000 W/m^2$) is the nominal irradiation.

$$I_s = I_{sn} \left(\frac{T_n}{T} \right)^3 \exp \left[\frac{qE_g}{ak} \left(\frac{1}{T_n} - \frac{1}{T} \right) \right] \quad (2.3)$$

Where E_g is the band gap energy of semiconductor ($E_g = 1.12 eV$ for Si) and I_{sn} is the nominal saturation current.

2.3.2 Single module ratings use for simulation

Solarex MSX60 parameters are taken from its datasheet for the simulation, that ratings are given below:

Table 2.1: Single Module Ratings

Peak power (P_{max})	60 W
Voltage @ peak power (V_{mpp})	17.1 V
Current @ peak power (I_{mpp})	3.5 A
Guaranteed minimum peak power	58 W
Open circuit voltage (V_{oc})	21.1 V
Short circuit current (I_{sc})	3.8 A
Temperature coefficient of voltage	$-(80 \pm 10) mV/^\circ C$
Temperature coefficient of current	$(0.0065 \pm 0.015) A/^\circ C$

2.3.3 Simulation results of one module

The electrical characteristics like $i - v$ and $p - v$ curve of the module are drawn at varying irradiance condition. We know the PV current changes with the solar irradiation level, and the PV output voltage changes with the temperature of the PV module, which is shown in the following simulation results. Here Figure 2.7(a) and Figure 2.7(b) show the $i - v$ and $p - v$ curve of a single PV module respectively, at different irradiance level. The $i - v$ or current-voltage curve mainly originates from the equation (2.1), as this equation represents the relation between PV current and PV voltage. At nominal irradiance level of the $i - v$ curve, when $i_{pv} = 0$, we will get the open circuit voltage (V_{oc}) of PV module and when $v_{pv} = 0$, we will get short circuit current (I_{sc}) of PV module. Similarly Figure 2.8(a) shows electrical characteristics like $i - v$ curve and Figure 2.8(b) shows the $p - v$ curve of a single PV module at different temperature condition. We usually take 1000 W/m^2 as nominal irradiance level and 25°C as the nominal temperature of the PV panel. So the simulation of standalone PV system is done at nominal temperature or at 25°C .

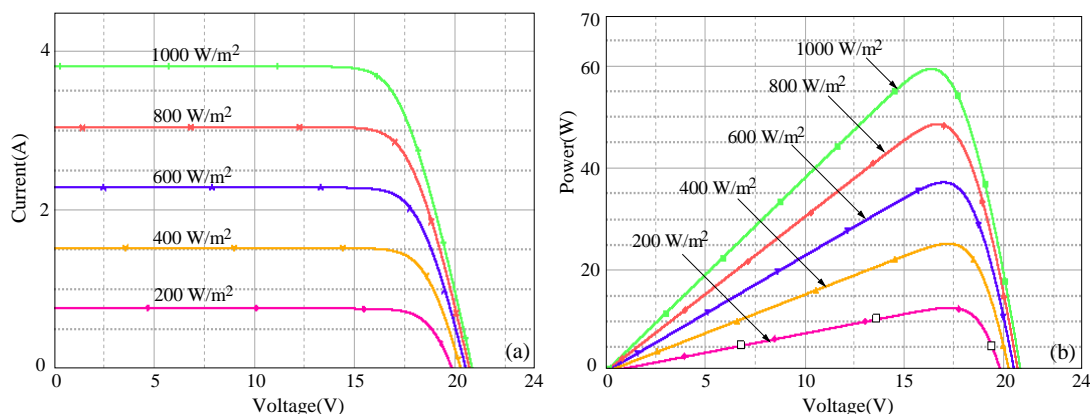


Figure 2.7: (a) $i - v$ curve (b) $p - v$ curve at different irradiance level

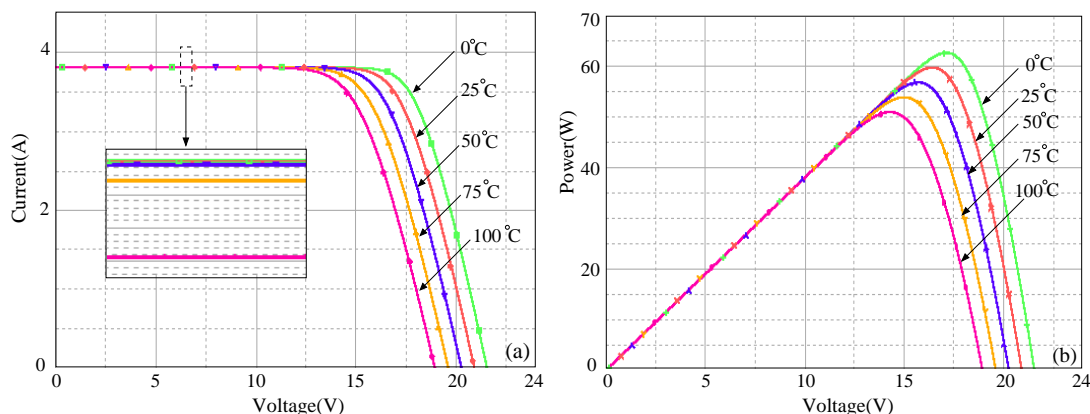


Figure 2.8: (a) $i - v$ curve (b) $p - v$ curve at different temperature level

2.4 Battery

Photovoltaic cells are used to convert solar energy into electrical energy. Solar energy is only available during day time and its intensity is affected by environmental condition such as cloudy weather etc. To overcome this issue, storage element is used to store solar energy whenever it is available in excess amount. Stored energy is utilized when solar power is not sufficient to supply load demand. Battery is most commonly used storage element as they store energy through an electrochemical process and thus have quick response in both charging and discharging processes. Also batteries have high power and energy density compared to other storage device like ultra-capacitors, compressed air systems, etc. The BSS can provide a flexible energy management solutions, which improves the power quality of the PV power generation system [18].

2.4.1 Battery Modeling

Modeling of Battery has very important role for simulation of the standalone PV system where it is used to maintain power balance between generation and demand. Generally battery can be modeled in three ways, such as experimental model, electrochemical model and equivalent circuit model. But for dynamic simulation equivalent circuit model is most suitable, which assumes that the battery is composed of a controlled-voltage source in combination with a series resistance as shown in Figure 2.9. In this work a generic battery model of lead-acid

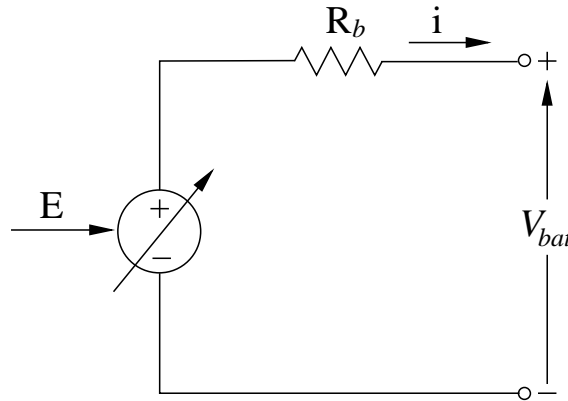


Figure 2.9: Battery equivalent circuit

battery is used as it is more convenient for renewable systems because of its low cost and availability in large size. By using the charging and discharging equation the lead-acid battery is modeled and this model is well accepted for use in simulation of renewable sources like PV system and also can be used in electric vehicle applications [10]. From the above equivalent circuit we can write; $V_{bat} = E - R_b \cdot i$, where

$$\text{For discharging : } E = E_0 - K \frac{Q}{Q - it} \cdot it - K \frac{Q}{Q - it} \cdot i^* + Exp(t) \quad (2.4)$$

$$\text{For charging : } E = E_0 - K \frac{Q}{Q - it} \cdot it - K \frac{Q}{it - 0.1 \cdot Q} \cdot i^* + Exp(t) \quad (2.5)$$

Where, V_{bat} is the actual battery voltage, E is the controlled voltage (V), i is the charging or discharging current of battery (A), R_b is the internal resistance of the battery (Ω), E_0 is the constant open circuit potential (V), i^* is the filtered battery current (A), $it = \int idt$ is the actual battery charge, K is the polarization constant (V/Ah), Q is the battery capacity (Ah), A is the exponential zone amplitude (V), and B is the exponential zone time constant inverse (Ah) $^{-1}$. This exponential zone can be represented by a non-linear dynamic equation;

$$\dot{Exp}(t) = B \cdot |i(t)| \cdot (-Exp(t) + A \cdot u(t)) \quad (2.6)$$

Here $Exp(t)$ =exponential zone voltage (V), $i(t)$ =battery current, $u(t)$ =charge or discharge mode ($u(t) = 0$ for discharge mode and $u(t) = 1$ for charge mode).

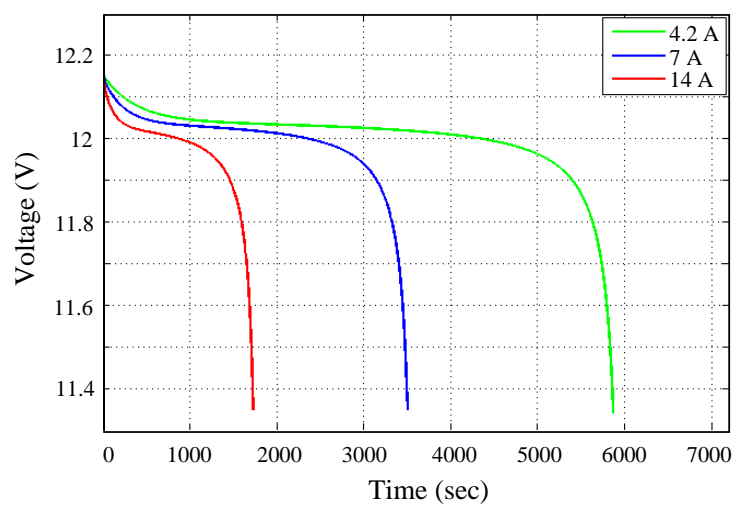


Figure 2.10: Simulation result of discharge characteristics

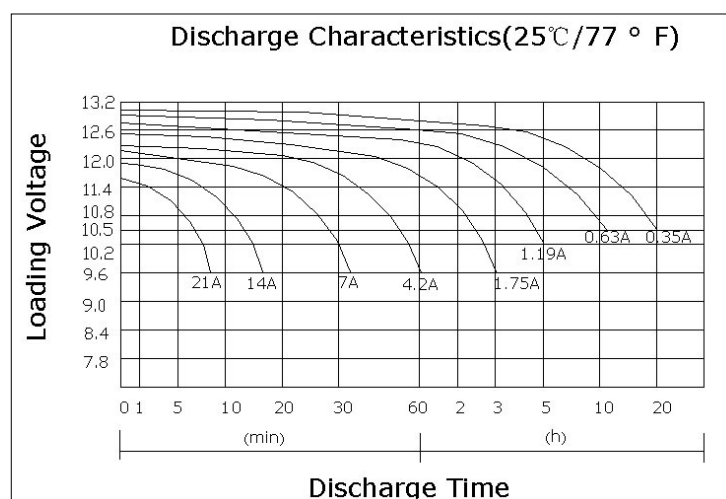


Figure 2.11: Data-sheet result of discharge characteristics

2.5 Boost Converter

Boost converter is a type DC to DC power converter in which output voltage is greater than its input voltage. It is one class of SMPS which contains at least two semiconductors, a diode and a MOSFET/transistor and two energy storage element, a capacitor and an inductor. Its input has an inductor which reduces the input current ripple and filter capacitor is normally placed at the output of the boost converter to reduce output voltage ripple. A Boost converter is also called as step-up converter as it is used to step up the voltage level with the same input power. The input power mainly comes from any suitable DC sources, such as solar panels, batteries, and rectifiers. Since in all systems power ($P = VI$) must be conserved, the output current of boost converter is lower than that of the input or source current. This converter is widely used in solar applications as this increases the voltage level of solar power and for this the number of solar cells reduces. Nowadays MPPT technique is used to increase the conversion efficiency by extracting maximum available power of the PV module, where boost converter is dominantly used. This MPPT controller switches the MOSFET of the boost converter by producing the control gate pulse.

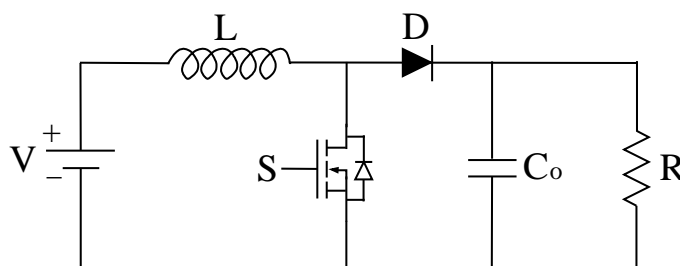


Figure 2.12: Boost or Step-up Converter

2.6 Bidirectional DC DC converters

Mainly in bidirectional DC DC converter, power can flow in both the directions. This type of converters are mainly used in the system that contains battery, fuel cell and ultra-capacitor, where there is a chance of bidirectional power flow. Basically, bidirectional DC DC converters can be divided into two categories depending on the Galvanic isolation between the input and output side [19]:

1. Non-isolated bidirectional DC DC converters
2. Isolated bidirectional DC DC converters

Basically a non-isolated bidirectional DC DC converter can be derived from the unidirectional DC DC converters by enhancing the unidirectional conduction capability of the conventional converters by the bidirectional conducting switches. Due to the presence of the diode in the basic buck and boost converter circuits, they do not have the inherent property of the bidirectional power flow. This limitation in the conventional Boost and Buck converter circuits can be removed

by introducing a power MOSFET or an IGBT having an antiparallel diode across them to form a bidirectional switch and hence allowing current conduction in both directions for bidirectional power flow in accordance with the controlled switching operation. The above circuit can be made to work in buck or boost

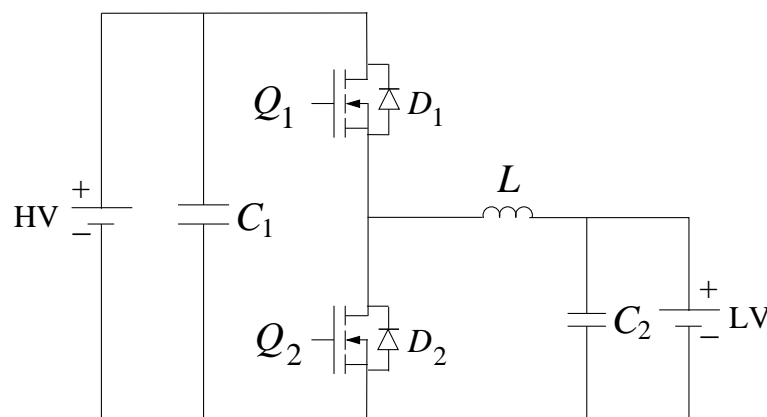


Figure 2.13: Non-isolated bidirectional buck-boost converter

mode depending on the switching of the MOSFETs Q_1 and Q_2 . The switches Q_1 or Q_2 in combination with the anti-parallel diodes D_1 or D_2 (acting as freewheeling diode) respectively, makes the circuit step up or step down the voltage applied across them. The bidirectional operation of the above circuit can be explained in the below two modes as follows:

Mode 1 (Boost Mode): In this mode switch Q_2 and diode D_1 enters into conduction depending on the duty cycle whereas the switch Q_1 and diode D_2 are off all the time. This mode can further be divided into two interval depending on the conduction on the switch Q_2 and diode D_1 .

Interval 1: (Q1-off, D1-off; Q2-on, D2-off) In this mode Q_2 is on and hence can be considered to be short circuited, therefore the lower voltage battery charges the inductor and the inductor current goes on increasing till not the gate pulse is removed from the Q_2 . Also since the diode D_1 is reversed biased in this mode and the switch Q_1 is off, no current flows through the switch Q_1 .

Interval 2: (Q1-off, D1-on; Q2-off, D2-off) In this mode Q_2 and Q_1 both are off and hence can be considered to be opened circuited. Now since the current flowing through the inductor cannot change instantaneously, the polarity of the voltage across it reverses and hence it starts acting in series with the input voltage. Therefore the diode D_1 is forward biased and hence the inductor current charges the output capacitor C_1 to a higher voltage. Therefore the output voltage boosts up.

Mode 2 (Buck Mode): In this mode switch Q_1 and diode D_2 enters into conduction depending on the duty cycle whereas the switch Q_2 and diode D_1 are off all the time. This mode can further be divided into two interval depending on the conduction on the switch Q_2 and diode D_1 .

Interval 1: (Q1-on, D1-off; Q2-off, D2-Off) In this mode Q1 is on and hence can be considered to be short circuited. The higher voltage battery will charge the inductor and the output capacitor will get charged by it.

Interval 2: (Q1-off, D1-off; Q2-off, D2-on) In this mode Q2 and Q1 both are off. Again since the inductor current cannot change instantaneously, it gets discharged through the freewheeling diode D2. The voltage across the load is stepped down as compared to the input voltage.

2.7 Single Phase Inverter

A inverter is a device that converts DC power into corresponding AC power. Mainly single phase inverter is of two types:

1. Single phase voltage source inverter (VSI)
2. Single phase current source inverter (CSI)

Single phase VSI is mainly used for converting DC power into AC power. To provide the electrical power to any load or appliances, the inverter converts the DC bus voltage to a single phase AC voltage with appropriate amplitude and frequency. The DC side voltage of a single phase VSI is kept constant by connecting a huge capacitor in parallel to the input voltage. So VSI has low input impedance as input has a bulk capacitor and it produces voltage of square wave or quasi-square wave. The AC side current is fixed up by the load connected at the output of the VSI. Anti-parallel diodes are used in single phase VSI to provide energy feedback path and are called as feedback diodes or freewheeling diodes. The single phase VSI circuit has direct control over the output voltage. Again single phase VSI can be divided in to two types [20];

- Half bridge inverter
- Full bridge inverter

2.7.1 Half bridge inverter

Half bridge inverter mainly consists of two switches S1 and S2 along with two anti-parallel diodes. This switches may be thyristor, BJT, IGBT or MOSFET, which depends on the power and frequency of operation. Here two equal capacitors C1 and C2 of are connected in series across the input voltage that divides the input DC voltage into two equal halves across each capacitor. The switch S1 and S2 operates in complementary mode i.e. when S1 is in on state, S2 is off and vice-versa.

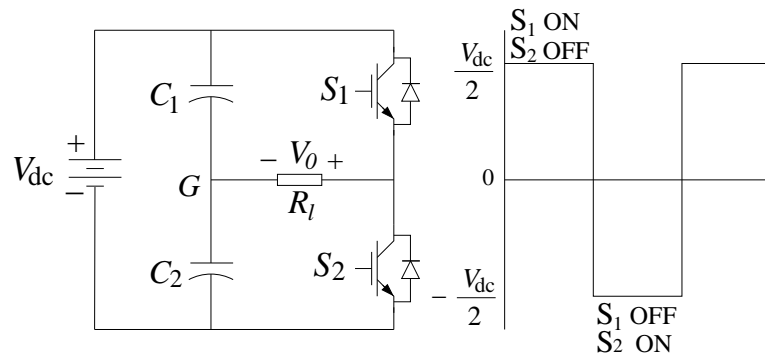


Figure 2.14: Single phase half bridge inverter

2.7.2 Full bridge inverter

Full Bridge inverter has four switches along with four anti-parallel diodes across each switch and that switch can be a BJT, MOSFET or IGBT. With the same input voltage, the maximum output voltage of the full bridge VSI is twice that of the output voltage of half bridge VSI. In the first half cycle switches S_1 and S_2 act simultaneously and during this time switches S_3 and S_4 are in completely off state. After 180° phase delay switches S_3 and S_4 are turned on and the previously on S_1 and S_2 are turned off. So we can say the operation of the switches pair (S_1, S_2) and (S_3, S_4) are complementary. Anti-parallel diodes will come into action when the load is inductive. When load will be inductive, current can not be suddenly comes to zero at the load and anti-parallel diodes provide the energy feedback path. In case of single phase CSI input current is kept constant

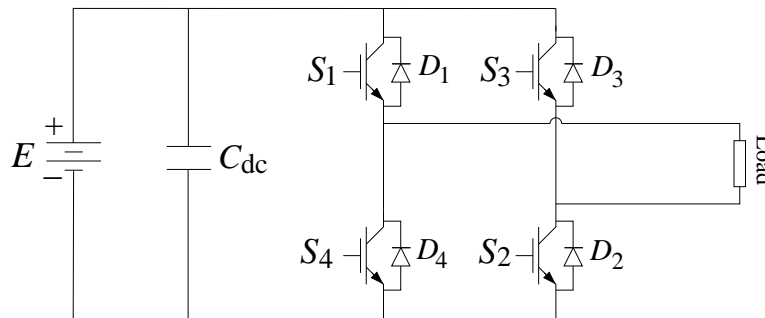


Figure 2.15: Single phase full bridge VSI

by connecting a large inductor in series with the input DC source. So CSI has high input impedance, as large inductor is connected to the input and here the AC side current is quasis-square wave. Like current in VSI, AC side voltage is determined or fixed up by the load connected to the output. Here anti-parallel diodes may or may not be needed. For other power semiconductor devices, sometimes series diodes are needed to block reverse voltage. The CSI circuit has direct control over the output current.

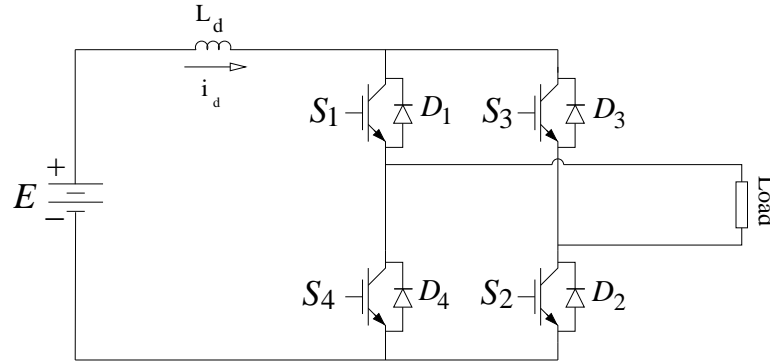


Figure 2.16: Single phase full bridge CSI

2.8 Filter

Nowadays, the use of renewable energy source is rapidly increasing in the modern distribution networks because of the disadvantages of the non-renewable energy sources. But renewable energy sources need inverter for interfacing with the utility grid. The switching frequency of these inverters is very high and which may introduce high order harmonics that can interfere with neighborhood EMI sensitive loads or equipment which are connected to the grid. Selecting a higher value of line-side inductance can be a solution, but, this will increase the cost of the system and gives the sluggish response. On the other hand, choosing an LCL-filter configuration permits the reduction of the inductance value and minimizing the switching frequency pollution emitted into the grid. An LC low-pass filter is generally connected at the output of the inverter to minimize the high frequency harmonics component. In certain applications like UPS, where pure sine wave is essential, good filtering is must. Here the inverter output voltage is a square wave which gives zero average value and it contains large number of harmonics. So to find the sine wave from this high frequency square wave, we have used a LC low-pass filter with a damping resistance shown in Figure 2.17. In our simulation the inductor and capacitor values of the LC filter are taken as $L_f = 2.7 \text{ mH}$ and $C_f = 10 \mu\text{F}$ respectively. Here the damping resistance value is taken as $R_d = 5 \Omega$.

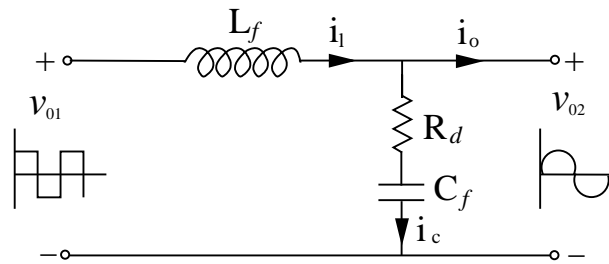


Figure 2.17: LC filter with damping resistance

2.9 Sinusoidal Pulse Width Modulation (SPWM)

The output voltage of an inverter can be regulated by regulating the gate pulse applied to the gate of the switch of the inverter. This is the commonly used method of regulating the output voltage and this method is named as Pulse Width Modulation (PWM) Control. It is also called as carrier based PWM technique. In this modulation process, there are multiple numbers of pulses per half cycle and the width of the pulses are different. Each pulse width is changing in according to the amplitude change of the sine wave, which is a control wave. The gate pulses are obtained by comparing a sinusoidal control signal with a high frequency triangular carrier signal. It is mainly of two types, such as unipolar and bipolar. Here for switching the inverter of standalone PV system bipolar PWM technique [20] is used and its mechanism is shown in Figure 2.18. In bipolar PWM technique, a control or desired signal is compared with a high frequency triangular wave to produce the desired switching pulses.

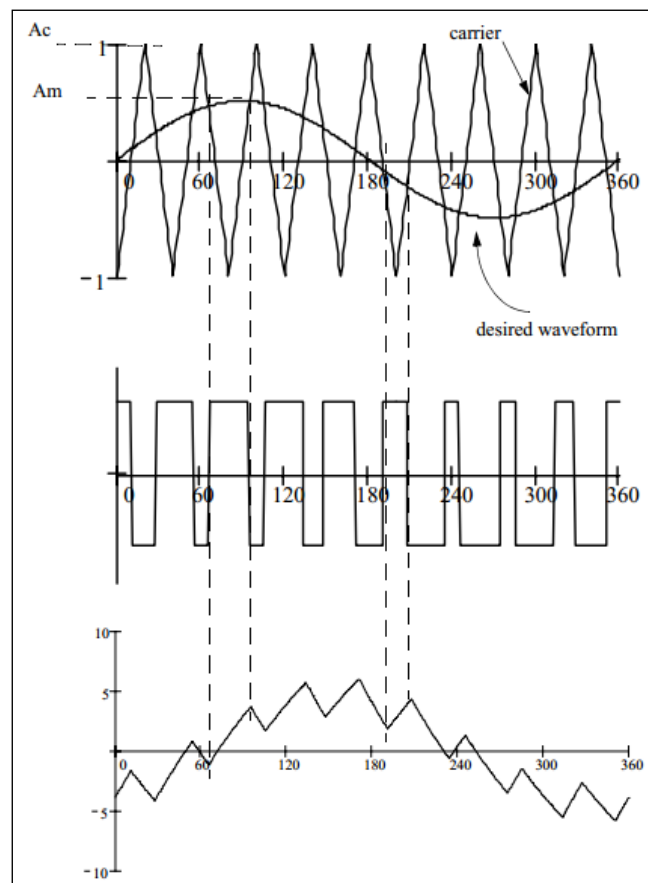


Figure 2.18: Bipolar sinusoidal pulse width modulation

2.10 Load

An electrical load is an electrical component that consumes electric power. Load can also be a portion of electrical circuit. Every device draws current that uses electricity to do work. The characteristics of a “Load” can vary widely. Examples of loads are resistor, light bulb, or motor. So we can say electrical load is a part of circuit that converts electricity in to heat, light or mechanical motion. The electrical loads can be classified into various categories as follows:

- According to load nature-1
 1. Resistive electrical loads.
 2. Inductive electrical loads.
 3. Capacitive electrical loads.
 4. Combination electrical loads.
- According to load nature-2
 1. Linear electrical load.
 2. Non-Linear electrical load.
- According to load function
 1. Lighting load.
 2. General / Small appliances load.
 3. Power loads.

2.11 Summary

This chapter has introduced photovoltaic system and discussed about the type of PV systems used. It has also discussed about the PV array, battery and their modeling. It has briefly described the components of the standalone PV system and discussed about the power converters and inverters involved in the system. Specially the structure and working of bidirectional buck-boost converter is discussed. Finally, this chapter completed with the discussion of the SPWM technique, LC-filter and load or appliances.

Chapter 3

Control Strategies and Analysis

Chapter 3

Control Strategies and Analysis

3.1 Overview

The chapter 3 gives us the idea about various control strategies involved and their analysis. For controlling the standalone PV system three independent control loops are used such as, analog MPPT control, battery control and inverter control. Section 3.2 describes the details about the analog MPPT technique and its working. Also this section gives clear idea about its stability, fastness and robustness behavior. Section 3.3 describes about the battery control technique and also this section describes about the state-space averaging of bidirectional buck-boost converter. The stability analysis of this battery control loop through bode diagram is done in the same section. In Section 3.4, the inverter control technique is described and in the same section the stability analysis of inverter control loop is described by bode diagram. In this section also brief description about the state-space averaging of single phase inverter is presented before doing its stability analysis.

3.2 Analog MPPT Control

The maximum power of the PV module changes with external climate conditions. At any operating condition there is only one value of current (I_{mpp}) and one value of voltage (V_{mpp}), that defines the maximum power point (MPP) at which power is maximum (P_{max}), as shown in Figure 3.1 [15]. We know the PV current changes with the solar irradiation level, and the PV output voltage changes with the temperature of the PV module. To increase the efficiency of PV array maximum power should be extracted from it. The MPPT control technique allows us to extract the maximum available power from the PV module in any operating condition. So inspired by this recent development, a control strategy for extracting maximum power from a PV array was derived. And this control strategy completely implemented using nonlinear dynamics principles. It is designed in such a way that the MPP becomes a global attractor of the system. Hence, under transient and steady state conditions the system will always converge upon the MPP irrespective of change to the operating conditions. This MPPT technique is implemented by using a boost DC-DC converter, as in standalone PV

system it is required to increase the voltage level at the input of the inverter or DC-link capacitor.

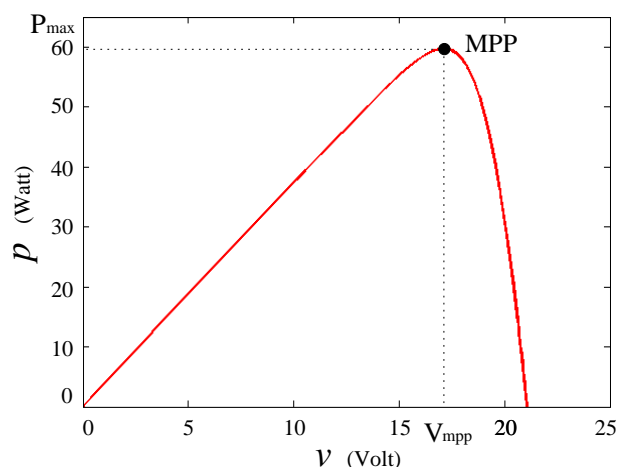


Figure 3.1: P-V curve.

Figure 3.2 shows a PV system block diagram with the proposed analog MPPT controller. This system consists of a PV module, a boost converter comprising of an input filter capacitor C , an inductor L , output filter capacitor C_{dc} , a diode and a controllable switch, regulated by the analog MPPT controller. Here PV module is connected to boost converter along with the analog MPPT controller to regulate the voltage and current of the PV module such that it will operate at MPP by continuously adjusting converter duty cycle. Solar cells show a unique global point at which power is maximum, shown in Figure 3.1 [21]. Denoting v and i as the module voltage and current respectively, the array's $v - p$ characteristics exhibits a unique global maximum at the point denoted by (V_{mpp}, P_{max}) , where $v = V_{mpp}$. So the the power p will be maximum at the operating array voltage, $v = V_{mpp}$. Unfortunately, the fundamental problem is that V_{mpp} is an unknown variable.

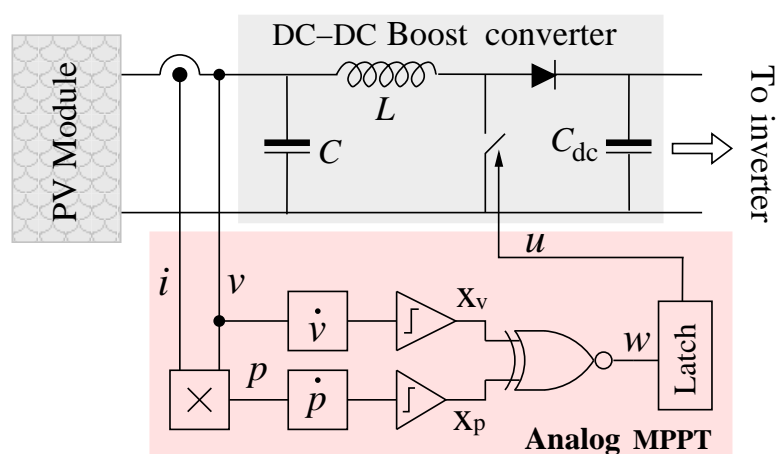


Figure 3.2: Analog MPPT controller with boost converter

3.2.1 Control Logic

As we know the array power p is a function of many variables i.e. $p = p(v, \theta_1, \theta_2, \dots)$ where θ 's represent such time varying parameters as temperature, illumination and aging etc, which cause p to vary. This leads to a equation given by

$$\frac{dp}{dt} = \frac{\partial p}{\partial v} \frac{\partial v}{\partial t} + \frac{\partial p}{\partial \theta_1} \frac{\partial \theta_1}{\partial t} + \frac{\partial p}{\partial \theta_2} \frac{\partial \theta_2}{\partial t} + \dots \quad (3.1)$$

In the above expression the parameters denoted by the θ 's introduce a noise term which is always a varying quantity to be considered. So V_{mpp} can not be deduced exactly. It is observed from the $v - p$ curve that MPP is located at $\partial p / \partial v = 0$ and mathematically, this can be expressed as

$$\frac{\partial p}{\partial v} = \begin{cases} > 0 & \text{when } v < V_{mpp} \\ = 0 & \text{when } v = V_{mpp} \\ < 0 & \text{when } v > V_{mpp} \end{cases} . \quad (3.2)$$

So an obvious control strategy would be

- (a) if $\partial p / \partial v > 0$, we deduced that $v < V_{mpp}$, so increase v towards V_{mpp} .
- (b) if $\partial p / \partial v < 0$, we deduced that $v > V_{mpp}$, so decrease v towards V_{mpp} .
- (c) if $\partial p / \partial v = 0$, we deduced that $v = V_{mpp}$, thus hold v constant, since operation is at the MPP.

So this ensures when $v < V_{mpp}$, then v should increase and thus its rate of change is positive and if $v > V_{mpp}$, then v is forced to fall and hence its rate of change should be negative. But if $v = V_{mpp}$, then v should held fixed, thus its rate of change should be zero. The above conclusions can be thus written as mathematical expression of v in differential form with respect to its position relative to V_{mpp} , such as :

$$\frac{dv}{dt} = \dot{v} = \begin{cases} > 0 & \text{when } v < V_{mpp} \\ = 0 & \text{when } v = V_{mpp} \\ < 0 & \text{when } v > V_{mpp} \end{cases} . \quad (3.3)$$

Irrespective of any initial voltage of PV module, the MPPT controller continuously forces the system's state trajectory to move towards the MPP to satisfy this conditions, that can be described by a simple function, $\dot{v} = -\gamma(v - V_{mpp})$. Where γ is a positive number and defines the dynamic response of the MPPT controller. Larger the value of γ , faster the speed of response. From the above discussion we can formulate a simple control law by taking $\dot{v} \propto \frac{\partial p}{\partial v} = k \frac{\partial p}{\partial v}$ (where k is a positive constant). Now, by substituting this control law into the expression $\frac{dp}{dt} = \frac{\partial p}{\partial v} \frac{dv}{dt}$, we can easily formulate the control equation $\frac{\partial p}{\partial v} = \dot{p} / \dot{v}$ with a control algorithm $\dot{v} = k \dot{p} / \dot{v}$, which is to be realised here. Practically realization of the algorithm $\dot{v} = k \dot{p} / \dot{v}$ is little bit difficult as \dot{v} appears on both sides and also divider circuit causes imperfect operations and singularity problem when \dot{v} becomes zero (when $v = V_{mpp}$). By rearranging also we can not realize $\dot{v}^2 = k \dot{p}$, as due to squaring it

will destroy the vital sign information. The control equation can be resolved as its RHS term \dot{p}/\dot{v} signifies its sign only. So to avoid the problem like singularity and use of divider circuit, author in [22, 23] redefined the control law, $\frac{\partial p}{\partial v} = \dot{p}/\dot{v}$ as

$$\frac{\partial p}{\partial v} = Sgn(\dot{p}/\dot{v}) \equiv \frac{Sgn(\dot{p})}{Sgn(\dot{v})} \equiv Sgn(\dot{p})Sgn(\dot{v})$$

$$\text{where } Sgn(X) = \begin{cases} +1 & \text{if } X > 0 \\ -1 & \text{if } X \leq 0 \end{cases}$$

Practically it is more convenient to use the boolean 0/1 instead of -1/+1 for representing the sign of a value. Thus, comparators are then used for evaluating its sign by producing binary signals, x_p and x_v for power and voltage respectively. The x_p value is 1 if $\dot{p} > 0$ or 0 if $\dot{p} \leq 0$ and x_v signal is treated same like x_p . And finally an XOR gate is used to multiply these two signs, which are now expressed as booleans or binary form. Then the exclusive-ORed output is sampled by a SR-latch with a constant clock frequency of $1/T$. Now whether the PV voltage should be increased or decreased to reach MPP is indicated by the signal w which drives the switch through latching circuit. When its value is 0, v should be increased and when it is 1, v should be decreased, which is described in a tabular form:

Table 3.1: Principle of operation of MPPT controller

Conditions	\dot{p}	\dot{v}	x_p	x_v	w	v
$v > V_{mpp}$	> 0	> 0	1	1	0	increases
		≤ 0	1	0	1	decreases
	≤ 0	≤ 0	0	0	0	increases
		> 0	0	1	1	decreases
$v \leq V_{mpp}$	≤ 0	> 0	0	1	1	decreases
		≤ 0	0	0	0	increases
	> 0	≤ 0	1	0	1	decreases
		> 0	1	1	0	increases

So in order to track the MPP, the controller should increase or decrease the voltage by switching the converter switch. When v decreases, the corresponding p also decreases, retreating from the MPP. To oppose this, the switch is opened by the MPPT controller. When the switch opens, C can charge and it will increase p by increasing v to approach the MPP as desired. However, it is not possible to reach the MPP exactly, because when $v = V_{mpp}$ the switch opens, increasing the

controls battery current against any parameter variations and the outer voltage loop regulates the DC bus voltage. The power balance between fluctuating solar power and time varying load is maintained by the battery charging or discharging process. When charging, switch Q1 is activated and the DC-DC converter works as a buck circuit, otherwise when discharging, switch Q2 activated and the DC-DC converter works as a boost circuit. When the DC-link voltage (V_{dc}) is greater than the reference voltage (V_{dcref}), switch Q1 is activated to run the circuit as a buck converter and when the DC-link voltage (V_{dc}) is lower than the reference voltage (V_{dcref}), switch Q2 is activated to run circuit as a boost converter. So the switch Q1 and Q2 activates in complimentary way (either buck mode or boost mode). The control strategy for buck-boost converter is shown in Figure 3.3. From this figure it is clear that there are two power MOSFETs in the configuration of converter in which both operates in complimentary way generated signal by the control logic. The pulse driven by PWM signal are used to switch the complimentary way operated MOSFETs for buck or boost operation. The voltage V_{dc} is compared with a reference DC-link voltage V_{dcref} to get the error signal and this error signal is passed through the PI controller to produce I_{batref} . After that the I_{batref} is compared with the sensed battery current to get the error signal and the error obtained is compensated by the PI controller for getting a PWM signal as shown in the Figure 3.3. The PWM signal or control signal is compared with a high frequency triangular signal to get the switching pulses. The switching frequency of this DC-DC converter is taken as 20 kHz. The PI controller parameters for voltage loop are $K_p = 0.08$ and $K_i = 5$ and for current loop are $K_p = 0.1$ and $K_i = 0.05$.

3.3.1 State-Space Averaging of Bidirectional Buck-Boost Converter

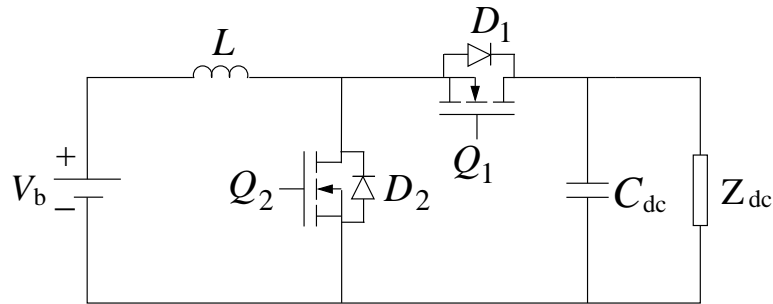


Figure 3.4: Equivalent circuit of PV module

For state-space modeling of bidirectional DC-DC converter we have considered the circuit shown in figure 3.4. It works mainly in two modes, buck mode and boost mode as discussed earlier. Again this two modes have four subinterval, depending on the diodes and MOSFETs turn on and turn off state. But from the four states of this circuit, two states are identical with other two. So for state-space modeling following two states are taken, which depends on the ON/OFF state of the MOSFETs.

Q2-on, Q1-off: In the first subinterval, when the switch Q1 is off and Q2 is on, the converter equivalent circuit can be represented in Figure 3.5. From the circuit we can write the state equations by using basic circuit laws, where inductor current i_l and capacitor voltage V_{dc} are the state variables.

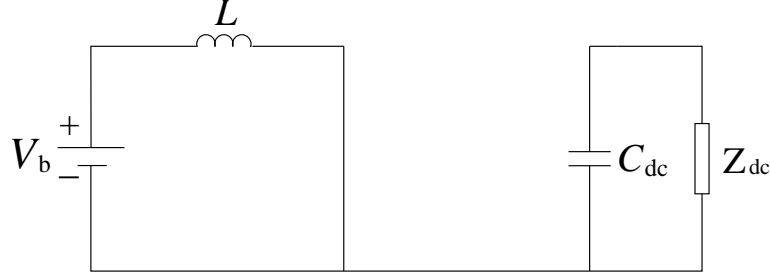


Figure 3.5: Equivalent circuit with Q1-off, Q2-on

$$\frac{di_l}{dt} = \frac{V_b}{L} \quad (3.4)$$

$$\frac{dV_{dc}}{dt} = \frac{-V_{dc}}{Z_{dc}C_{dc}} \quad (3.5)$$

Therefore the state-space equations for the first interval t_{ON} can be written as follows

$$\begin{aligned} \dot{X} &= A_{ON}X + B_{ON}U \\ Y &= C_{ON}X + D_{ON}U \end{aligned} \quad (3.6)$$

Where, $X = \begin{bmatrix} i_l \\ V_{dc} \end{bmatrix}$, $Y = V_{dc}$, $U = V_b$, $A_{ON} = \begin{bmatrix} 0 & 0 \\ 0 & -1/Z_{dc}C_{dc} \end{bmatrix}$,
 $B_{ON} = \begin{bmatrix} 1/L \\ 0 \end{bmatrix}$, $C_{ON} = [0 \ 1]$, $D_{ON} = 0$

Q1-on, Q2-off: In the second subinterval, when the switch Q1 is on and Q2 is off, the converter equivalent circuit can be represented in Figure 3.6. Similarly here also from the circuit we can write the state equations, where inductor current i_l and capacitor voltage V_{dc} are the state variables.

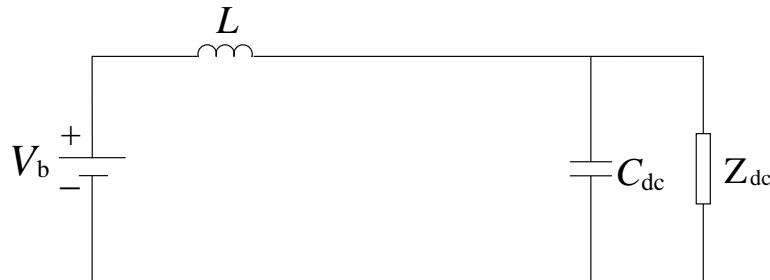


Figure 3.6: Equivalent circuit with Q1-on, Q2-off

$$\frac{di_l}{dt} = \frac{V_b}{L} - \frac{V_{dc}}{L} \quad (3.7)$$

$$\frac{dV_{dc}}{dt} = \frac{i_l}{C_{dc}} - \frac{V_{dc}}{Z_{dc}C_{dc}} \quad (3.8)$$

Therefore the state-space equations for the second interval t_{OFF} are as follows

$$\begin{aligned} \dot{X} &= A_{OFF}X + B_{OFF}U \\ Y &= C_{OFF}X + D_{OFF}U \end{aligned} \quad (3.9)$$

Where,

$$A_{OFF} = \begin{bmatrix} 0 & -1/L \\ 1/C_{dc} & -1/Z_{dc}C_{dc} \end{bmatrix}, \quad B_{OFF} = \begin{bmatrix} 1/L \\ 0 \end{bmatrix}, \quad C_{OFF} = [0 \quad 1], \quad D_{OFF} = 0$$

During each subinterval, since all the circuit parameters are constant, therefore equivalent circuit of the converter acts like a time invariant system. But during switching between the two modes, the converter behaves like a time variant system. Therefore the state-space averaging is used with respect to the corresponding time periods of both the subintervals so as to approximate the converter to the continuous time nonlinear time invariant system. After this, the nonlinear system is linearized about the operating point so as to get the continuous time linear time invariant system.

$$\begin{aligned} \frac{dx(t)}{dt} &= (d(t)A_{ON} + (1 - d(t)A_{OFF}))x(t) + (d(t)B_{ON} + (1 - d(t)B_{OFF}))u(t) \\ y(t) &= (d(t)C_{ON} + (1 - d(t)C_{OFF}))x(t) + (d(t)D_{ON} + (1 - d(t)D_{OFF}))u(t) \end{aligned} \quad (3.10)$$

The following linearized (ac, small-signal) system can now be obtained from (3.10)

$$\begin{aligned} \frac{d\hat{x}(t)}{dt} &= A\hat{x}(t) + H\hat{d}(t) \\ \hat{y}(t) &= C\hat{x}(t) \end{aligned} \quad (3.11)$$

Applying Laplace transform to above equation

$$\begin{aligned} \hat{x}(s) &= (sI - A)^{-1}H\hat{d}(s) \\ \hat{y}(s) &= C\hat{x}(s) \end{aligned} \quad (3.12)$$

where, $A = A_{ON}D + A_{OFF}D'$, $C = C_{ON}D + C_{OFF}D'$, $D' = 1 - D$ and $H = (A_{ON} - A_{OFF})X + (B_{ON} - B_{OFF})U$. Now we can extract the following transfer functions from the equation (3.12)

$$\frac{\hat{i}_l(s)}{\hat{d}(s)} = \frac{V_{dc}Z_{dc}C_{dc}s + V_{dc} + D'Z_{dc}i_l}{LC_{dc}Z_{dc}s^2 + Ls + D'^2Z_{dc}} \quad (3.13)$$

$$\frac{\hat{V}_{dc}(s)}{\hat{i}_l(s)} = \frac{Z_{dc}V_{dc}D' - LZ_{dc}i_l s}{V_{dc}Z_{dc}C_{dc}s + V_{dc} + D'Z_{dc}i_l} \quad (3.14)$$

Let us take

$$G_{ild}(s) = \frac{\hat{i}_l(s)}{\hat{d}(s)} \quad (3.15)$$

And as per our controller setting, we can write the current loop and voltage loop controller as follows

$$G_{i1}(s) = 0.1 + \frac{0.05}{s} \quad (3.16)$$

$$G_{v1}(s) = 0.08 + \frac{5}{s} \quad (3.17)$$

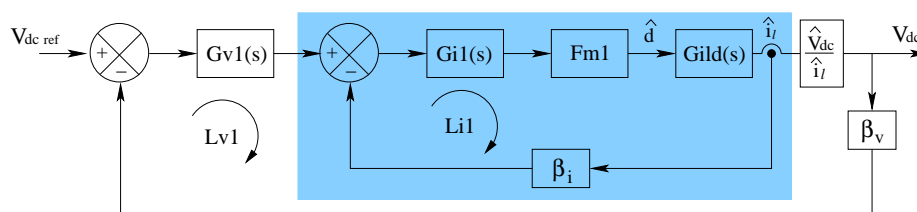


Figure 3.7: Control block diagram for battery

In the control block diagram shown in Figure 3.7, $F_{m1} = 1$ is the gain of PWM and $\beta_v = 0.06$, $\beta_i = 0.02$ are the voltage and current sensor gains respectively. Putting all the Transfer functions we can find the current loop gain $Li1$. And by plotting the bode diagram of current loop gain $Li1$, we find that the current loop is stable (see Figure 3.8). Also in similar manner we can find voltage loop gain $Lv1$ and its bode diagram shown in Figure 3.9. Both the inner and outer control loops are stable for our controller tuning parameter. The inner current loop $Li1$ has infinite gain margin and phase margin of 89.9 deg. Similarly the outer voltage loop $Lv1$ has gain margin of 50.3 dB and phase margin of 82.8 deg.

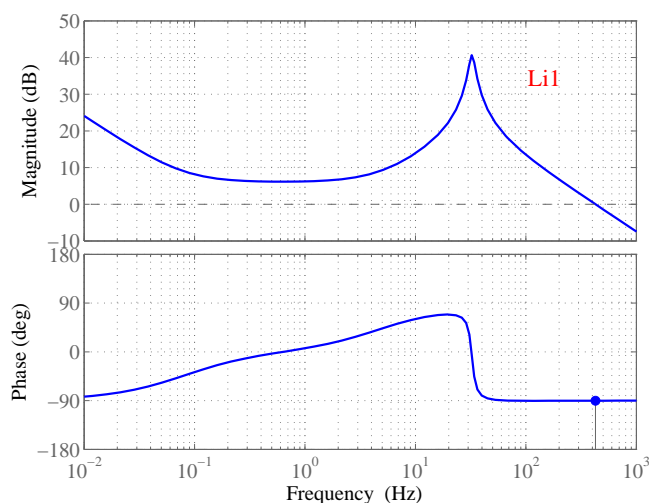


Figure 3.8: Bode diagram for current loop ($Li1$) of buck-boost converter

inductor and capacitor, R_L is the value of load resistor, β_v and β_i are feedback coefficients of output voltage and inductor current respectively. The feedback coefficients β_v and β_i are also known as sensor gains whose values are 0.06 and 0.02 respectively. The PI controller parameters are $K_{i1} = 1000$ for voltage loop and $K_{p2} = 4.22$, $K_{i2} = 100$ for current loop. The filter inductor L_f and capacitor C_f are taken as 2.7 mH and $10 \text{ } \mu\text{F}$ respectively for the system simulation. In LC-filter a damping resistance (R_d) of $5 \text{ } \Omega$ is taken. The switching frequency of this inverter is 16 kHz .

3.4.1 State-Space Averaging of Inverter

For states-space averaging of single phase inverter, first we need to do its states-space modeling. States-space modeling of inverter is done by considering the circuit shown in Figure 3.10. In a single phase inverter at a time two switches turn on and other two are at offstate and when other two turn on then the first switch comes to off state. So the the operation cycle of a single phase inverter can be considered in to two subinterval. Thus when switches S1 and S2 are on (S3 and S4 are off) are taken as first subinterval called t_{ON} and when switches S3 and S4 are on (S1 and S2 are off) are taken as second subinterval called t_{OFF} . The state equations of the single phase inverter are given below.

t_{ON} :

$$\frac{di_{lf}}{dt} = \frac{V_{dc}}{L_f} - \frac{v_0}{L_f} \quad (3.18)$$

$$\frac{dv_{cf}}{dt} = \frac{i_{lf}}{C_f} - \frac{v_0}{R_l C_f} \quad (3.19)$$

Therefore the state-space equations for the first interval t_{ON} can be written as follows

$$\begin{aligned} \dot{X} &= A_{ON}X + B_{ON}U \\ Y &= C_{ON}X + D_{ON}U \end{aligned} \quad (3.20)$$

Where, $X = \begin{bmatrix} i_{lf} \\ v_0 \end{bmatrix}$, $Y = v_0$, $U = V_{dc}$, $A_{ON} = \begin{bmatrix} 0 & -1/L_f \\ 1/C_f & -1/R_l C_f \end{bmatrix}$,

$$B_{ON} = \begin{bmatrix} 1/L_f \\ 0 \end{bmatrix}, \quad C_{ON} = [0 \quad 1], \quad D_{ON} = 0$$

t_{OFF} :

$$\frac{di_{lf}}{dt} = \frac{-V_{dc}}{L_f} - \frac{v_0}{L_f} \quad (3.21)$$

$$\frac{dv_0}{dt} = \frac{i_{lf}}{C_f} - \frac{v_0}{R_l C_f} \quad (3.22)$$

Therefore the state-space equations for the second interval t_{OFF} are as follows

$$\begin{aligned} \dot{X} &= A_{OFF}X + B_{OFF}U \\ Y &= C_{OFF}X + D_{OFF}U \end{aligned} \quad (3.23)$$

Where,

$$A_{OFF} = \begin{bmatrix} 0 & -1/L_f \\ 1/C_f & -1/R_l C_f \end{bmatrix}, \quad B_{OFF} = \begin{bmatrix} -1/L_f \\ 0 \end{bmatrix}, \quad C_{OFF} = [0 \quad -1], \quad D_{OFF} = 0$$

Similarly by using equation (3.12) and considering the effect of R_d , we can extract the following transfer functions

$$\frac{\hat{i}_{lf}(s)}{\hat{d}(s)} = \frac{2V_{dc} \cdot ((R_l + R_d) \cdot C_f s + 1)}{(R_l + R_d) \cdot C_f L_f s^2 + (L_f + R_l R_d C_f) \cdot s + R_l} \quad (3.24)$$

$$\frac{\hat{v}_0(s)}{\hat{i}_{lf}(s)} = \frac{R_l \cdot (1 + R_d C_f s)}{1 + (R_l + R_d) \cdot C_f s} \quad (3.25)$$

Let us take

$$G_{ilfd}(s) = \frac{\hat{i}_{lf}(s)}{\hat{d}(s)} \quad (3.26)$$

And as per our controller setting, we can write the current loop and voltage loop controller as follows

$$G_{i2} = 4.22 + \frac{100}{s} \quad (3.27)$$

$$G_{v2} = \frac{1000}{s} \quad (3.28)$$

Here we have assumed second order Pade's approximation in the inner loop ($Li2$), given as

$$D_{d2}(s) = \frac{1 - \frac{s \cdot T_d}{2} + \frac{(s \cdot T_d)^2}{12}}{1 + \frac{s \cdot T_d}{2} + \frac{(s \cdot T_d)^2}{12}} \quad (3.29)$$

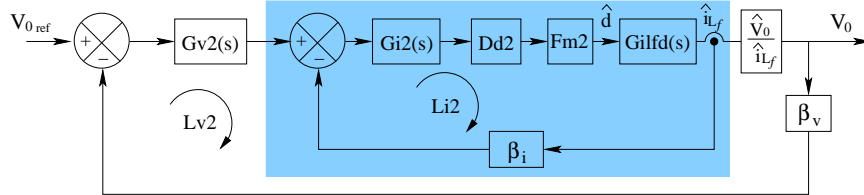
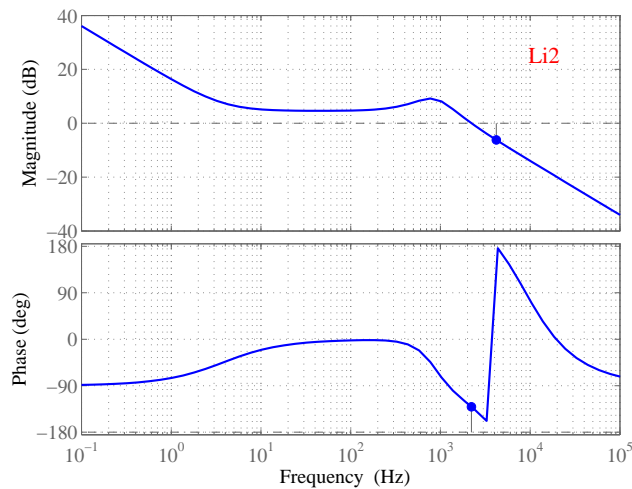
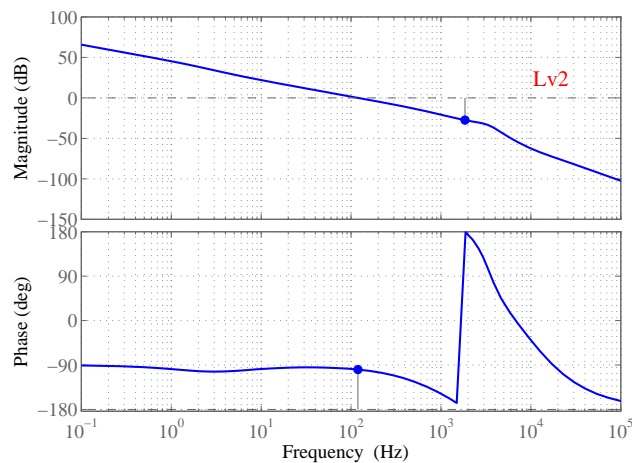


Figure 3.11: Control block diagram for inverter

In the control block diagram shown in Figure 3.11, $F_{m1} = 1$ is the gain of PWM and $\beta_v = 0.06$, $\beta_i = 0.02$ are the voltage and current sensor gains respectively. Putting all the Transfer functions we can find the current loop gain $Li2$. And by plotting the bode diagram of current loop gain $Li2$, we find that the current loop is stable (see Figure 3.12). Also in similar manner we can find voltage loop gain $Lv2$ and its bode diagram shown in Figure 3.13. Both the inner and outer control loops are stable for our controller tuning parameter. The inner current loop $Li2$ has gain margin of 6.5 dB and phase margin of 48.9 deg. Similarly the outer voltage loop $Lv2$ has gain margin of 27.5 dB and phase margin of 80.8 deg.

Figure 3.12: Bode diagram for current loop ($Li2$) of inverterFigure 3.13: Bode diagram for voltage loop ($Lv2$) of inverter

3.5 Summary

This chapter has introduced three control strategies used in this work. It has discussed about the control strategies indivisually. First the analog MPPT control is described and its tracking control logic is analysed. Secondly the battery control strategy is discussed and its stability analysis is done by extracting transfer functions using the state-space averaging technique for bidirectional buck-boost converter. Bode plot analysis is presented for the battery control loops, which are stable for our tuning value of controller parameters. At last the current control strategy for inverter is discussed which is required for maintaining a stable voltage and current at the output. Later the stability analysis ia also done for inverter control loop by extracting transfer functions using the state-space averaging technique for inverter. It concluded with the bode plot analysis of the inverter control loops, which are stable for our controller parameters setting.

Chapter 4

Results and Discussion

Chapter 4

Results and Discussion

4.1 Overview

The chapter 4 contains the simulation results of the system and discussion about it. Section 4.2 gives a brief idea about the simulation of the standalone PV system and its parameter values. The results and discussion is presented in Section 4.3. This section is divided into three subsections. The first subsection shows the steady state result at nominal condition, where battery has no role to play and its discussion. In second subsection the results are given under load variation at constant source power and its discussion for the result is done there only. In the last subsection the results are shown under PV power variation by varying the solar irradiance. At that time the output load power is kept constant and its discussion is presented for the simulation results.

4.2 Simulation

In a standalone PV system, battery is used as backup source to provide stable voltage and current to the load. Stable voltage and current at the load can be achieved when the PV generated power should be balanced with the load demand power. That means when PV generation is less than the load demand, battery needs to provide the extra power and when PV generation is more than the load demand, battery needs to store the extra power. Battery is a bidirectional device as it can store and give energy by its charging and discharging process respectively. So in this research work, the standalone PV system is simulated and the simulation results show the effectiveness of all the three control loops used. And simulation results also show the purpose of using BSS in the standalone PV system, which satisfies the objectives of this work mentioned in the chapter 1.

For Simulation of this standalone PV system a 2 kW PV generation is taken, where $N_s=9$ and $N_p=4$ are considered during PV modeling. That means the 60 W module we have simulated, are taken nine module in one row having four rows total. BSS is nothing but a pack of batteries connected in parallel or series manner. In our simulation we have taken lead-acid battery pack in which 8 numbers of 12 V batteries are connected in series. 7 Ah is the standard 12 V lead-acid battery

capacity, taken from data-sheet of Shimastu NP7-12. In this simulation no parallel connection is done that means the battery capacity remains unchanged. But if we want large capacity of BSS, then we need to connect them in parallel fashion and for increasing the voltage rating of the BSS we to increase the battery connection in series. Here in our simulation the BSS voltage rating is 96 V, for that reason 8 numbers of 12 V batteries are connected in series. The inductor and capacitor values of the LC filter connected at the output of single phase inverter are taken as $L_f = 2.7 \text{ mH}$ and $C_f = 10 \text{ } \mu\text{F}$ respectively. There we have taken the damping resistance value as $R_d = 5 \text{ } \Omega$. The DC-link capacitor (C_{dc}) and inductor (L) of buck-boost converter are taken as $2000 \text{ } \mu\text{F}$ and 2 mH respectively for the simulation. In this work for simulation we have considered the resistive load only.

4.3 Results and Discussion

4.3.1 At nominal condition

First let us assume that the PV power generation is equal to the load demand power, and at that time battery is not supplying or taking any power. In our system at nominal condition PV system produces 2 KW of electrical power.

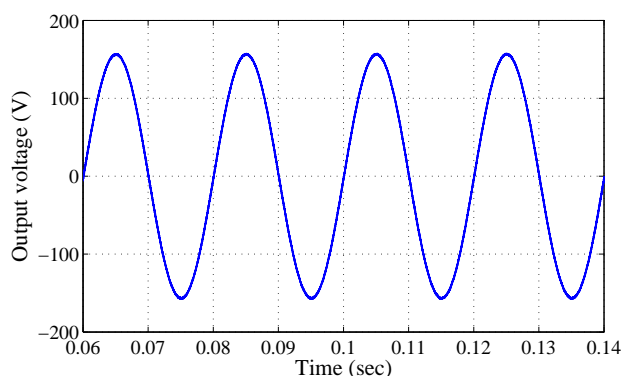


Figure 4.1: Steady state output voltage (V_0)

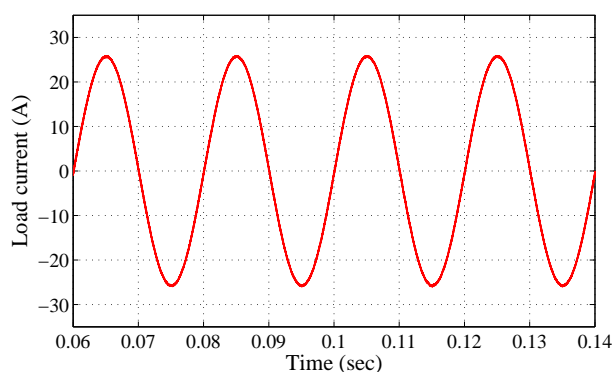


Figure 4.2: Steady state load current (i_0)

At this condition the standalone PV system is simulated and its steady state output voltage (v_0) and load current (i_0) are shown in Figure 4.1 and Figure 4.2 respectively. This shows the controlling action of the inverter control system. The steady state dc-link voltage is shown in Figure 4.3 along with its reference value. Its proper tracking shows the effectiveness of the battery control by the bidirectional DC-DC converter. The steady state result of V_{mpp} and I_{mpp} are also shown in Figure 4.5 and Figure 4.6 respectively at nominal condition. These two results signify the working and effectiveness of analog MPPT controller. At this time as battery is not storing or giving any power through its charging and discharging process, its SOC curve remains constant throughout shown in Figure 4.4.

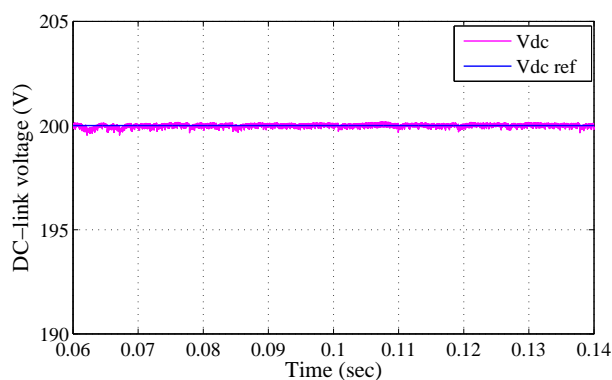
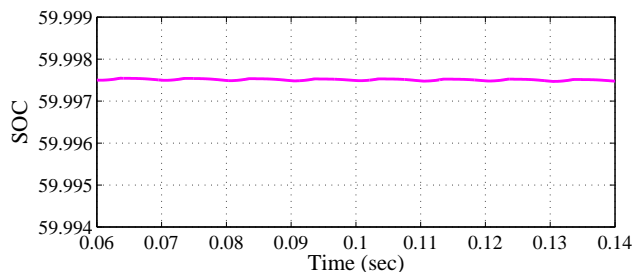
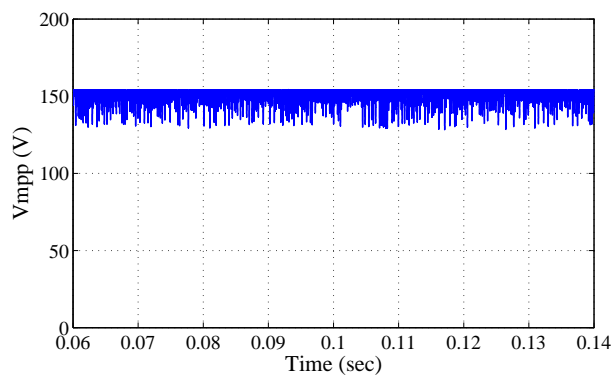
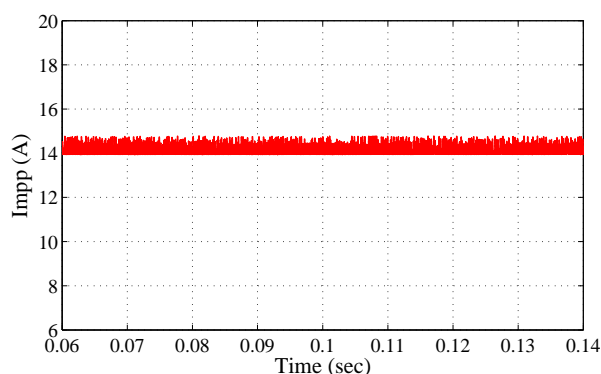
Figure 4.3: Steady state DC-link voltage (V_{dc})

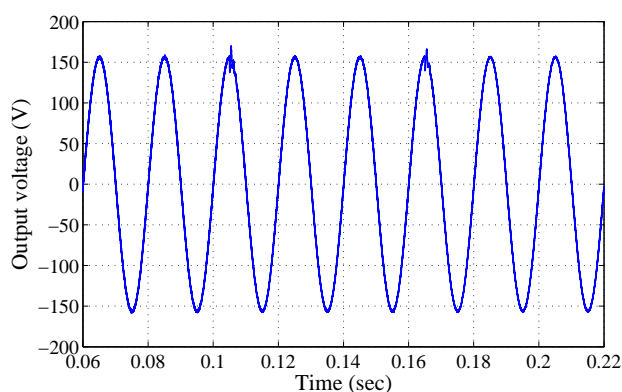
Figure 4.4: Steady state SOC of battery system

Figure 4.5: Steady state PV voltage at MPP (V_{mpp})

Figure 4.6: Steady state PV current at MPP (I_{mpp})

4.3.2 With load variation

As in standalone system solar energy is the only source of energy, battery system is used to mitigate the load demand. Some times when solar energy production is low the battery system can provide the excess energy demanded by the load. When load varies there will be a power mismatch between solar generation and local load, and that power gap can be fulfilled by the use the lead-acid battery system. When load increases the battery have to supply the extra power and when load decreases the battery have to consume this extra power. Here a resistive load is taken for siulation and it is varied like the following $7.5 \Omega \rightarrow 6 \Omega \rightarrow 5 \Omega$, and the simulation results are captured for output voltage, load current, battery's SOC and powers at generation and demand. In other words active power load is varied in the following sequence, $1.6 kW \rightarrow 2 kW \rightarrow 2.4 kW$. For this load variation the steady state output voltage is shown Figure 4.7, which indicates that under load variation the output voltage is remains unchange and stable. This proves the effectiveness of inverter current control technique which is responsible for maintaining 110 V of constant voltage across the load. The output load current

Figure 4.7: Output voltage (V_0) under load variation

wave form is shown in Figure 4.8 under the same load variation. From the output current result it is clear about the load variation, as the load current changing after some specified time. But this current waveform has less transient effect which

signifies the stability of inverter control loop. From the power curves shown in

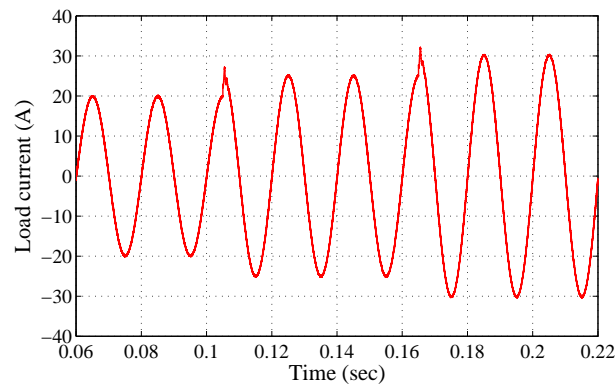


Figure 4.8: Load current (i_0) under load variation

Figure 4.9, it is clear that when PV generation is greater than load power demand, battery starts charging and its SOC increases and when load power demand is more than the PV generation, battery discharges to provide the additional power to the load and its SOC starts decreasing. When the load power demand is same as the PV power generation, battery need not to take or give any power which keeps its SOC remains constant, shown in Figure 4.10. SOC curve shown in Figure 4.10 reflects the charging and discharging process of BSS according to the load power variation.

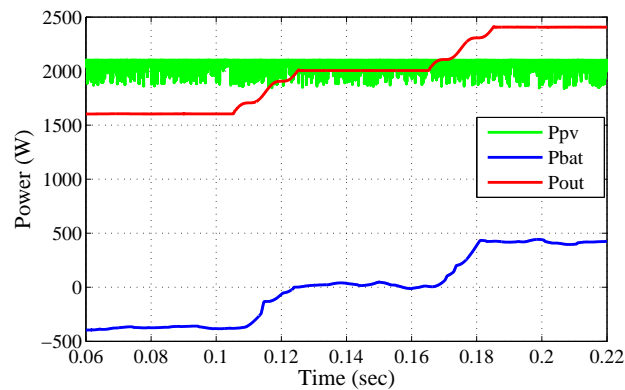


Figure 4.9: PV, output load and battery power under load variation

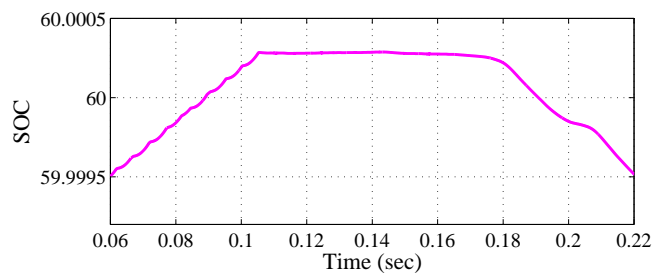


Figure 4.10: SOC of battery system under load variation

4.3.3 With solar irradiance variation

As we know solar power is intermittent in nature, it can not provide a steady power to the load connected. That means sometimes load power demand is constant, but due to the variation in solar power generation, we need the help of BSS to compensate that extra power. So when PV generation power is not sufficient to mitigate the load demand, BSS needs to provide the extra power through the discharging process and this condition is called underproduction. When PV generation power is more than the load power demand, the BSS needs to store the excess power through the charging process and this condition is called overproduction. Hence when there is overproduction, battery needs to charge and when there is underproduction, battery needs to discharge (see Figure 4.11). To verify this condition simulation results have been proposed.

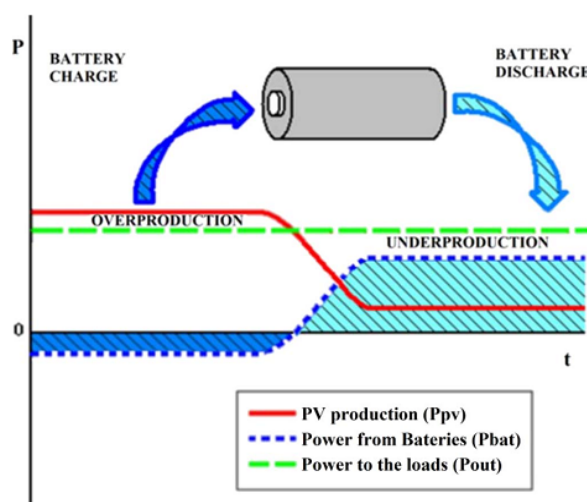


Figure 4.11: Power management protocol under solar irradiance variation

Figure 4.12 and Figure 4.13 show the output voltage and load current respectively under solar power variation. The voltage and current wave form are stable and transient free at the load, which shows the proper working of inverter control technique. Solar generated power is varied by varying its irradiance level in the following sequence $800 \text{ W/m}^2 \rightarrow 1000 \text{ W/m}^2 \rightarrow 1200 \text{ W/m}^2$. In Figure 4.14 the power curves are shown, which shows the PV power variation, output power and battery power variation. This power curves gives a clear view of the solar power variation. From this power curves it is clear that when solar power is less than the output power demand, BSS is providing the extra amount of power through discharging process and when solar power is greater than the output power demand, BSS is taking the extra amount of power through charging process. During discharging, battery power is positive and during charging its power is negative, which can be seen from the graph. The SOC curve shown in Figure 4.15, gives clear idea about battery charging and discharging process. The V_{mpp} and I_{mpp} curves are shown in Figure 4.16 and Figure 4.17 respectively.

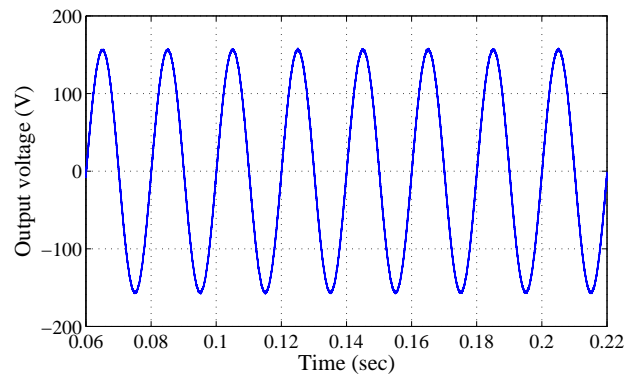
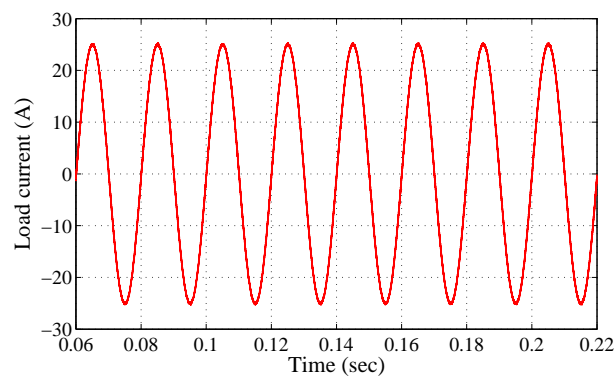
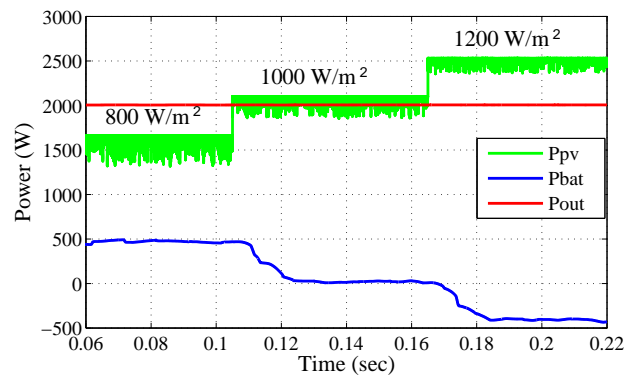
Figure 4.12: Output voltage (V_0) under solar irradiance variationFigure 4.13: Load current (i_0) under solar irradiance variation

Figure 4.14: PV, output load and battery power under solar irradiance variation

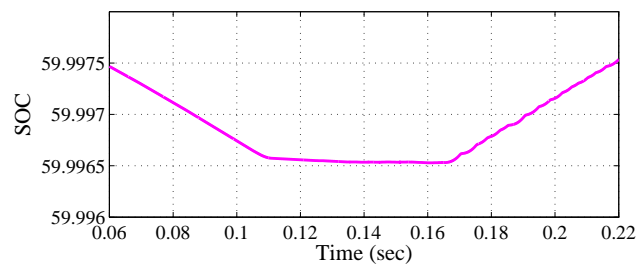


Figure 4.15: SOC of battery system under solar irradiance variation

The I_{mpp} curve also gives the clear idea about the solar power variation by varying its irradiance level, as solar irradiance has direct influence on PV current. The proposed analog MPPT controller is fast and robust, that can be seen from the I_{mpp} curve. It is properly tracking under solar irradiance variation and has very fast dynamic response. The solar power variation does not have any impact on the load voltage and current, as battery charging and discharging is capable of stabilizing the system. As solar irradiance change has very negligible effect on the MPPT voltage, V_{mpp} curve shows very less variation with respect to solar irradiance (see in Figure 4.16). From power curves, as initially the PV generated power is less than the load demand, the BSS is giving the extra amount of power by its discharging process. After that when solar energy is at nominal level battery need not to be discharged or charged, which is clearly shown by its SOC curve, in Figure 4.15. When the solar irradiance again increases, BSS starts charging to consume the extra amount of power and it stabilizes the system. This extra stored energy can be utilized when load demand will be more or solar irradiance will be less. So when BSS is discharging, SOC curve is going down and when BSS is charging, this curve is increasing with respect to time.

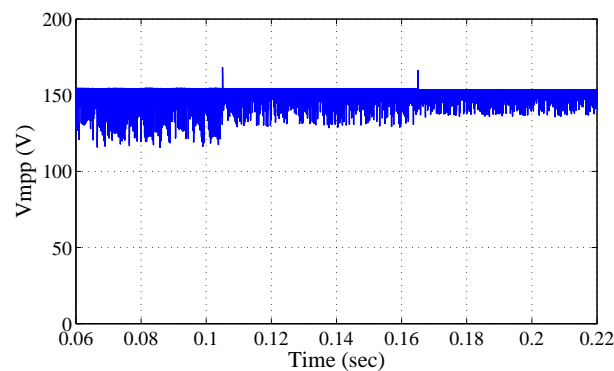


Figure 4.16: V_{mpp} under solar irradiance variation

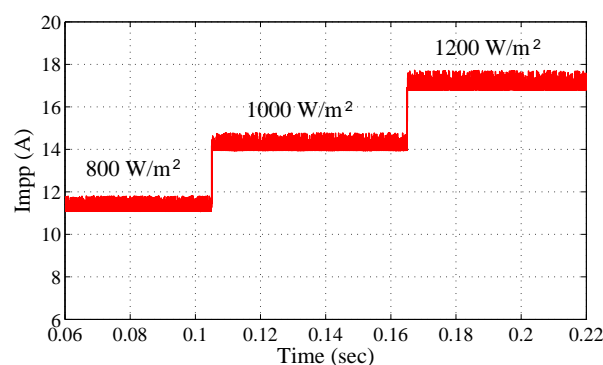


Figure 4.17: I_{mpp} under solar irradiance variation

4.4 Summary

This chapter described about the simulation of the standalone photovoltaic system and discussed about its results. The steady state simulation result are given and discussed at nominal condition. The objectives of this work are varified by giving proper simulation results. The simulation results of standalone PV system under load variation with constant solar power are shown and discussed. Also the simulation is done under source power variation at constant output load power and its results are ploted and discussed. Solar power variation is mainly done by varing the solar irradiation level at the constant temperature. All the results shown and discussed to fulfil and achieve of the objectives mentioned in the first chapter.

Chapter 5

Conclusion and Future Scope

Chapter 5

Conclusion and Future Scope

5.1 Overview

This chapter summarizes the complete work done in this research and gives an overall picture of the work and results achieved. Section 5.2 gives an overall conclusion and outlines the results of this thesis. Finally, Section 5.3 concludes with future research scope.

5.2 Conclusion

In this work, a standalone photovoltaic (PV) system is taken, in which a storage device is used as a backup source. The energy storage system is used to make the intermittent PV power more dispatchable and stable. Here, the storage device is mainly taken as lead-acid battery, as it is more convenient to use in high power applications such as solar and wind systems because of its low cost and availability in large size. Lead-acid battery is modeled by considering its charging and discharging equations based on the equivalent circuit. The dynamic behavior obtained in simulation is close to the actual behavior of lead-acid battery. It has been demonstrated that the constant current discharge curve obtained in simulation is close to the actual discharge behavior given in the data-sheet. PV system is also modeled by using its equivalent circuit and the equations involved, for the system simulation. In this work, three independent control loops are used for the standalone PV system. Those are MPPT control loop for extracting maximum power from PV module, battery control loop for bidirectional power flow between battery and DC bus through buck-boost converter and inverter control loop for maintaining stable voltage and current at local load. The analog MPPT controller is very robust and extracts the maximum power available at the solar panel. A bidirectional buck-boost DC-DC converter is used to maintain continuous power flow between the DC bus and BSS with a constant DC-link voltage. A constant DC-link voltage is maintained by charging or discharging the lead-acid battery depending on the load change or solar irradiance change. In this work a current-controlled single phase VSI with bipolar pulse width modulation is used to maintain the stable voltage and current at local load. The stability analysis is performed by using bode plots for both the inverter control loop and buck-boost

converter control loop and these control loops are stable for our tuned controller parameters. The purpose of using lead-acid battery in standalone PV system is verified by varying load power and solar irradiance level in the simulation. The simulation results in both the cases proves the effectiveness of the controllers. When the load power demand is more than the PV generation, the battery should provide the extra power and when PV generation is more than the load power demand, the battery should store the extra power. This proves the power balance condition of the system. This is achieved through proper charging and discharging control of Lead-acid battery by controlling the duty cycle of the bidirectional buck-boost converter. And also under sudden load variation the single phase VSI gives stable output voltage and current with very less transient variation. So the proposed control methods are working effectively on the standalone PV system with lead-acid battery as backup source.

5.3 Future Scope

The future research scopes are as follow:

1. The experimental set up will be developed to validate the effectiveness of the proposed controllers for standalone PV system.
2. The proposed work will be extended by connecting with the utility grid to exchange the power from PV source to grid and vice-versa.
3. The advanced control strategies like sliding mode control will be applied to the system dynamics for enhancing the system immunity to the parameter change and system disturbance.
4. A number of micro-sources are connected in parallel to form a microgrid. The load sharing among the sources is our future investigation.

5.4 Summary

This chapter concluded about the standalone PV system and discussed some of the future scope on research can be done. This work proposed three individual control loop for the standalone PV system. All the control loops are discussed and analysed properly. For inverter control loop and battery control loop stability analysis is done by using bode diagram, that gives clear idea about the system stability for this controller parameter tuning. As in islands and remote locations, standalone PV system a the optimal power solution, this work can be implemented for the society. And also the work done on standalone PV system will be a key motivation to work on a grid-connected PV system for future research.

Bibliography

- [1] H. Mahmood, D. Michaelson, and J. Jiang. A Power Management Strategy for PV/Battery Hybrid Systems in Islanded Microgrids. *IEEE Journal of Emerging and Selected Topics in Power Electronics*, 55(1):1–14, Jun. 2014.
- [2] H. Mahmood, D. Michaelson, and J. Jiang. Control Strategy for a Standalone PV/Battery Hybrid System. In *IECON 2012-38th Annual Conference on IEEE Industrial Electronics Society*, pages 3412–3418, 25-28 Oct. 2012.
- [3] W. A. Omran, M. Kazerani, and M. M. A. Salama. Investigation of Methods for Reduction of Power Fluctuations Generated From Large Grid-Connected Photovoltaic Systems. *IEEE Trans. Energy Convers.*, 25(1):318–327, Mar. 2011.
- [4] H. Fakham, D. Lu, and B. Francois. Power Control Design of a battery charger in a Hybrid Active PV generator for load-following applications. *IEEE Trans. Ind. Electron.*, 58(1):240–250, Jan. 2011.
- [5] R. Bhatt and B. Chowdhury. Grid frequency and voltage support using PV systems with energy storage. In *North American Power Symposium (NAPS)*, pages 1–6, 4-6 Aug. 2011.
- [6] S. Adhikari and L. Fangxing. Coordinated V-f and P-Q Control of Solar Photovoltaic Generators With MPPT and Battery Storage in Microgrids. *IEEE Trans. Smart Grid*, 5(3):1270–1281, May. 2014.
- [7] R.-J. Wai, W.-H. Wang, and C.-Y. Lin. High-Performance Stand-Alone Photovoltaic Generation System. *IEEE Trans. Ind. Electron.*, 55(1):240–250, Jan. 2008.
- [8] H.-L. Tsai, Ci-S. Tu, and Yi-J. Su. Development of Generalized Photovoltaic Model Using MATLAB/SIMULINK. In *World Congress on Engineering and Computer Science (WCECS)*, pages 1–6, 22-24 Oct. 2008.
- [9] J.B. Copetti and F. Chenlo. A general battery model for PV system simulation. *Journal of Power Sources*, 47:109–118, 1994.
- [10] O. Tremblay and L.-A. Dessaint. Experimental Validation of a Battery Dynamic Model for EV Applications. *World Electric Vehicle Journal*, 3:2032–6653, 2009.

-
- [11] O. Tremblay, L.-A. Dessaint, and A.-I Dekkiche. A Generic Battery Model for the Dynamic Simulation of Hybrid Electric Vehicles. In *Vehicle Power and Propulsion Conference 2007 VPPC IEEE*, pages 284–289, Sep. 2007.
- [12] Q. Bin and M. Yundong. Research on Control Strategies of a Stand-alone Photovoltaic System. In *International Conference on Renewable Energies and Power Quality (ICREPPQ12)*, pages 1–6, 28-30 Mar. 2012.
- [13] D. V. de la Fuente, C. L. T Rodriguez, G. Garcera, E. Figueres, and R.O. Gonzalez. Photovoltaic Power System With Battery Backup With Grid-Connection and Islanded Operation Capabilities. *IEEE Trans. Ind. Electron.*, 60(4):1571–1581, Apr. 2013.
- [14] Y. Ru, J. Kleissl, and S. Martinez. Storage Size Determination for Grid-Connected Photovoltaic Systems. *IEEE Trans. Sustainable Energy*, 4(1):68–81, Jan. 2013.
- [15] R. Gules, J. D. P. Pacheco, H. L. Hey, and J. Imhoff. A Maximum Power Point Tracking System With Parallel Connection for PV Stand-Alone Applications. *IEEE Trans. Ind. Electron.*, 55(7):2674–2683, Jul. 2008.
- [16] B. Yang, W. Li, Y. Zhao, and X. He. Design and Analysis of a Grid-Connected Photovoltaic Power System. *IEEE Trans. Power Electron.*, 25(4):992–1000, Apr. 2010.
- [17] M. G. Villalva, J. R. Gazoli, and E. R. Filho. Comprehensive approach to modeling and simulation of photovoltaic arrays. *IEEE Trans. Power Electron.*, 24(5):1198–1208, May. 2009.
- [18] X. Li, D. Hui, and X. Lai. Battery Energy Storage Station (BESS)-Based Smoothing Control of Photovoltaic (PV) and Wind Power Generation Fluctuations. *IEEE Trans. Sustainable Energy*, 4(2):464–473, Apr. 2013.
- [19] H. R. Karshenas, H. Daneshpajoo, A. Safaee, P. Jain, and A. Bakhshai. Bidirectional DC-DC Converters for Energy Storage Systems. In *Energy Storage in the Emerging Era of Smart Grids*, pages 161–177.
- [20] N. Mohan, T. M. Undeland, and W. P. Robbins. *Power Electronics : Converters, Applications, And Design*. John Wiley & Sons, 2011.
- [21] P. Midya, P. T. krein, R. J. Turnbull, and J. Kimball. Dynamic maximum Power Point Tracker for Photovoltaic Application. In *Proc. IEEE PESC'96*, pages 1710–1716, PP 1996.
- [22] Y. H. Lim and D. C. Hamill. Simple maximum power point tracker for photovoltaic arrays. *Electronics Letters*, 36:997–999, May 2000.
- [23] S. Maity and P. K. Sahu. Modeling and Analysis of a Fast and Robust Module-Integrated Analog photovoltaic MPP Tracker. *IEEE Trans. Power Electron.*, pages 1–11, Feb. 2015.

- [24] S.-K. Kim, J.-H. Jeon, C.-H. Cho, J.-B. Ahn, and S.-H. Kwon. Dynamic Modeling and Control of a Grid-Connected Hybrid Generation System With Versatile Power Transfer. *IEEE Trans. Ind. Electron.*, 55(4):1677–1688, Apr. 2008.

- [25] N. S. Jayalakshmi, D. N. Gaonkar, A. Balan, P. Patil, and S. A. Raza. Dynamic modeling and Performance Study of a Stand-alone Photovoltaic System with Battery Supplying Dynamic Load. *INTERNATIONAL JOURNAL of RENEWABLE ENERGY RESEARCH*, 4(3):635–640, May. 2014.